New precise measurement of the $e^+e^- \to \pi^+\pi^-(\gamma)$ *cross section with BaBar*

Léonard Polat

on behalf of the *BaBar* collaboration

leonard.polat@lphne.in2p3.fr

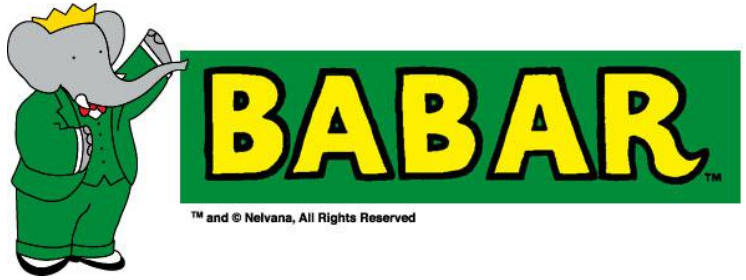

Rencontres de Moriond (Electroweak), 19/03/2026

Introduction

Hadronic vacuum polarization (HVP) contribution to the anomalous magnetic moment of the muon (a_μ) obtained by measuring cross section of $e^+e^- \to$ hadrons processes: largest input (73%) from $e^+e^- \to \pi^+\pi^-$.

Current tensions between:

- predictions from dispersion approach and direct measurement,
- predictions from dispersion approach and lattice QCD,

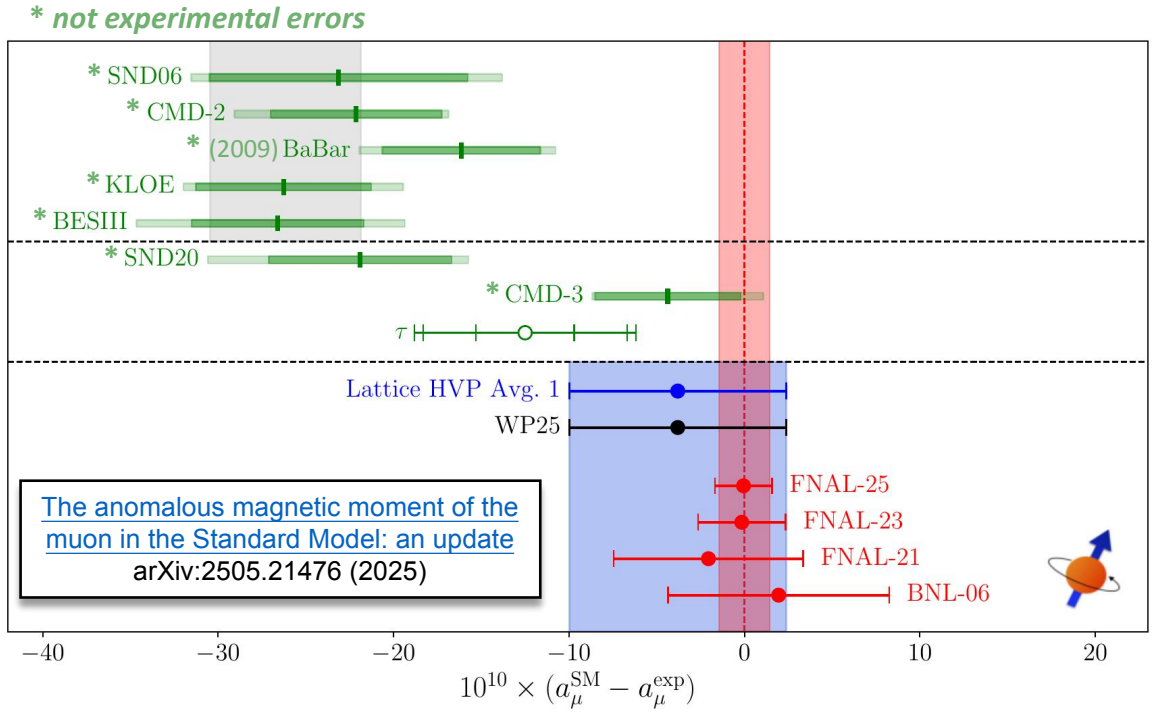

Introduction

Hadronic vacuum polarization (HVP) contribution to the anomalous magnetic moment of the muon (a_μ) obtained by measuring cross section of $e^+e^- \to$ hadrons processes: largest input (73%) from $e^+e^- \to \pi^+\pi^-$.

Current tensions between:

- predictions from dispersion approach and direct measurement,
- predictions from dispersion approach and lattice QCD,
- measurements from KLOE, BaBar and CMD-3 (*KLOE vs CMD-3*: > 5σ tension at *ρ* peak).

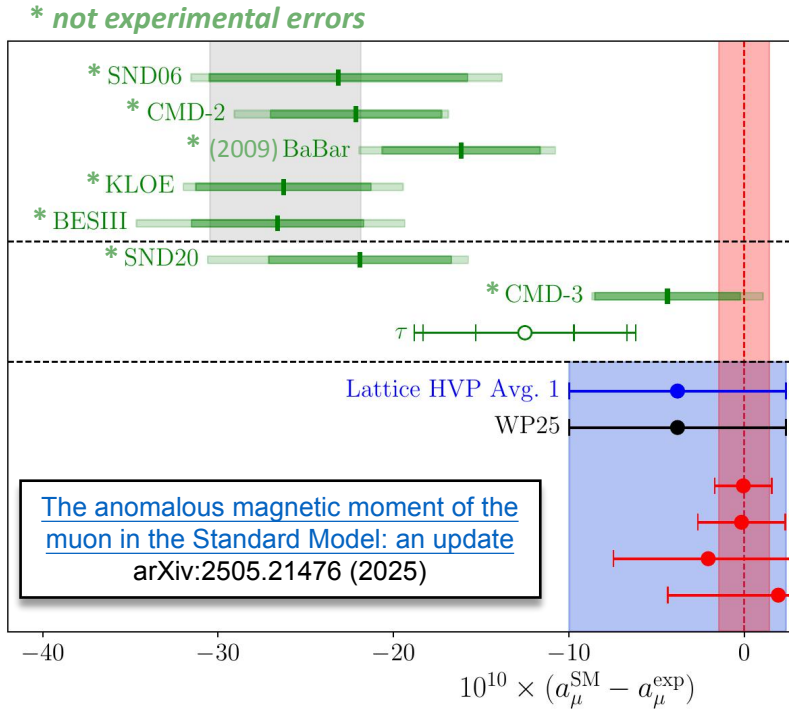

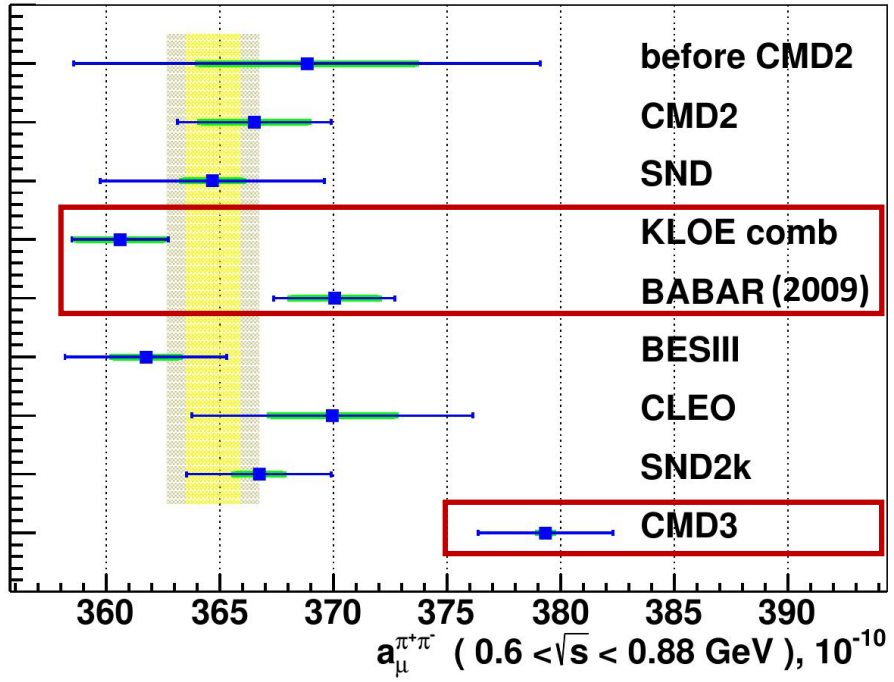

CMD-3 Collaboration
Measurement of the e+e−→π+π− cross section from threshold to 1.2 GeV with the CMD-3 detector
Phys. Rev. D 109, 112002 (2024)

Previous BaBar result from 2009 (partial data).

This talk: new BaBar measurement of the $e^+e^- \to \pi^+\pi^-(\gamma)$ cross section with full data samples, new & independent method aiming at improved precision.

The BaBar experiment & Simulation samples

PEP-II: asymmetric e^+ **(3 GeV)** – e^- **(9 GeV) collider** located at SLAC (USA).

Operated from 1999 to 2008 at $\Upsilon(4S/3S/2S)$ **resonance** energies.

Collected **424.2 fb^{-1} at** $\Upsilon(4S)$ ($\sqrt{s} = 10.58$ GeV) **+ 36.2 fb^{-1}** off-resonance.

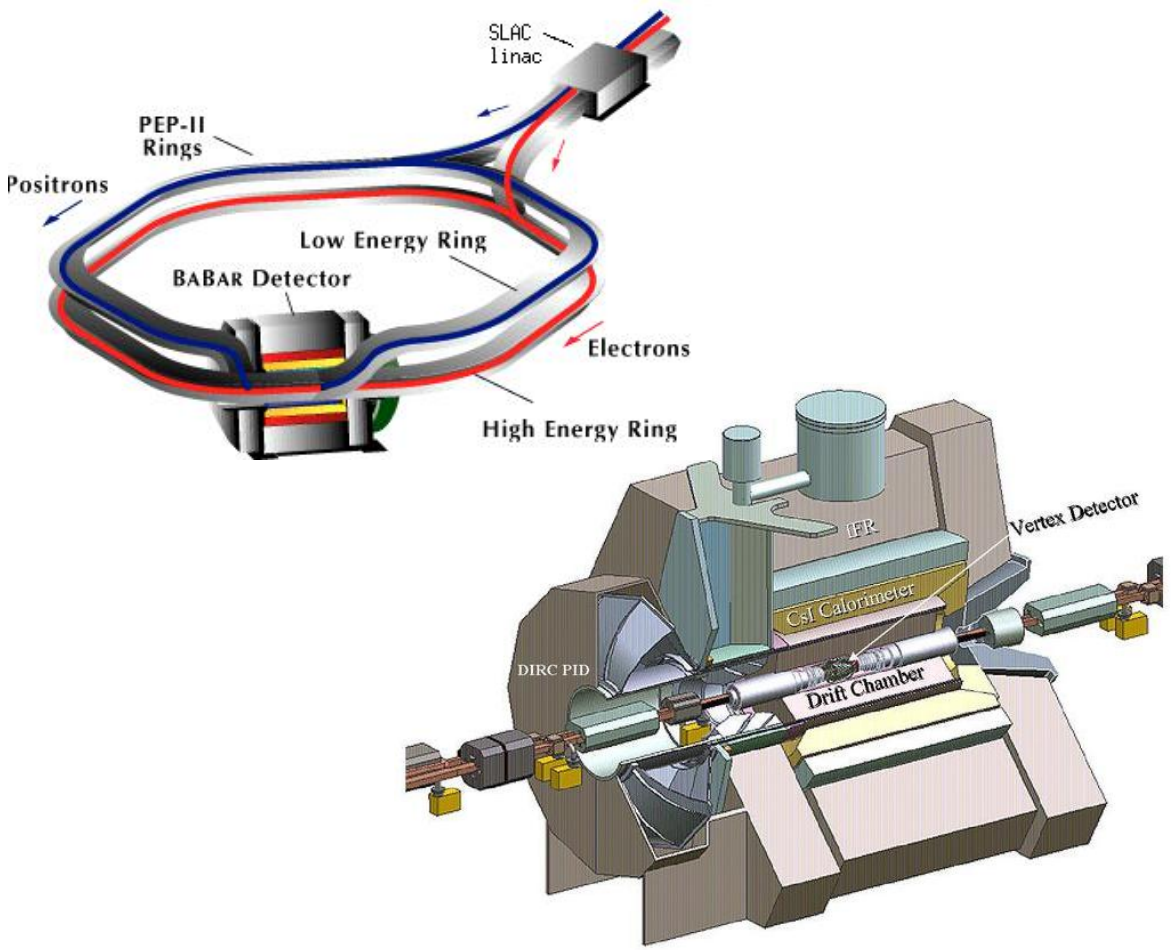

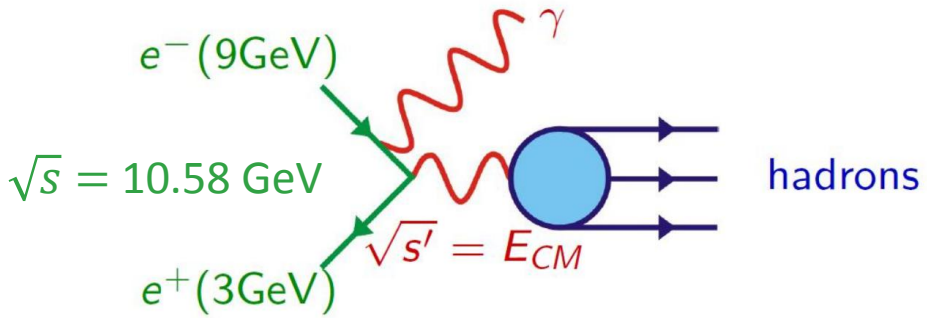

Initial state radiation (ISR) strategy: large range of center-of-mass energies probed after γ_{ISR} emission from e^+ or e^-.

Monte Carlo (MC) signals: $\boldsymbol{\pi^+\pi^-(\gamma)\gamma_{\mathrm{ISR}}}$ **&** $\boldsymbol{\mu^+\mu^-(\gamma)\gamma_{\mathrm{ISR}}}$ with *Phokhara9.1* generator.

MC backgrounds:

$e^+e^- \to K^+K^-(\gamma)\gamma_{\mathrm{ISR}}$, $q\bar{q}$ $(q = u, d, s, c)$, $\tau^+\tau^-$, $X\gamma_{\mathrm{ISR}}$ $(X = n\pi/K + m\pi^0, \ldots)$.

Differences between 2009 & 2025 measurements

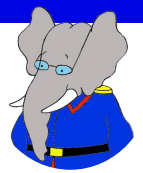

Previous analysis (2009): Phys. Rev. Lett. 103, 231801 – 2009 | Phys. Rev. D 86, 032013 – 2012

- Runs 1 to 4 (232 fb^{-1} at $\Upsilon(4S)$),
- π/μ separation using particle identification **(PID), dominant source of systematics**,
- Momentum selection on each track: $p > 1$ GeV/c (more reliable μID),
- Total relative systematic uncertainty ($0.5 - 1$ GeV/c^2) = **0.50%**.

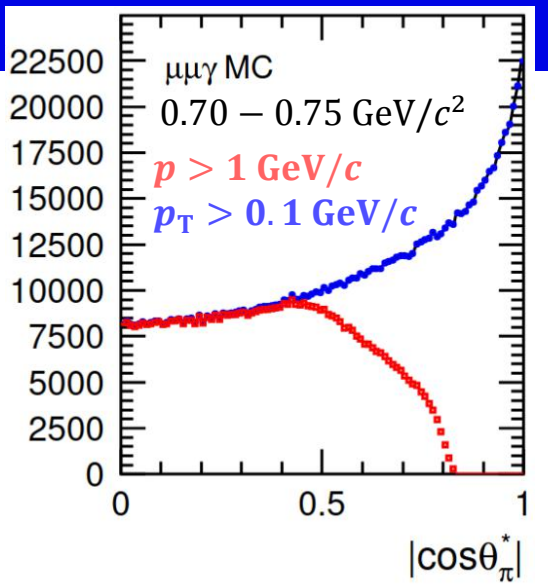

Current analysis (2025):

- **New method** proposed by M. Davier (2017) to separate processes in data instead of PID: angular fit of data over $|\cos\theta^*|$ (θ^* = angle between negative charged track and γ_{ISR} in 2-track CM frame),
- Separation between π/μ at large $|\cos\theta^*|$: release $p > 1$ GeV/c cut,
- Tracks down to $p_{\mathrm{T}} \sim 0.1$ GeV/c, runs 1-6 and **no PID requirement**: larger statistics, aiming at reduced syst. uncertainties.

→ **Independent method** to check the 2009 BaBar result. Also **blinded analysis**: offsets (constant multiplicative factors) applied on mass spectra at different steps.

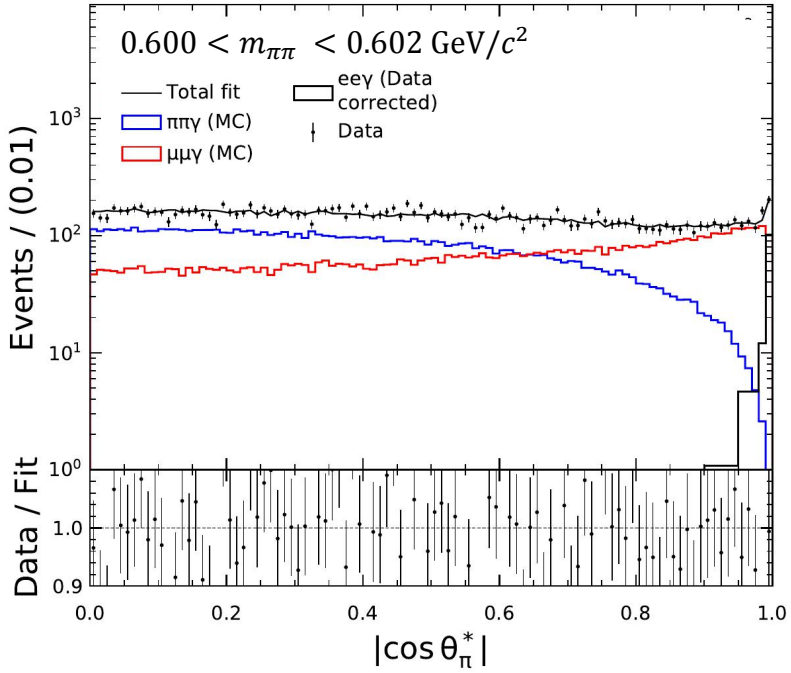

Overview of analysis steps

1. Kinematic fits of additional radiation → **2-dimensional selection** against background (*slide 7*).
2. **Angular fit** of data with data/MC corrections → $\pi\pi$ and $\mu\mu$ mass spectra (*slides 8 - 10*).

   ↪ **blinding** on absolute normalization of **tracking** corrections, **trigger** corrections and **fitted mass spectra**, independently for $\pi\pi$ and $\mu\mu$: **6 different blindings**.
3. Conclusive comparison of $\mu\mu$ spectrum shape vs simulation → **unblinding of $\boldsymbol{\mu\mu}$** to compare normalization to **QED prediction** (*slide 11*).
4. Successful QED test → $\mu\mu$ spectrum unfolded to $\sqrt{s'}$, i.e. center-of-mass energy of final state including FSR → **ISR luminosity** (*slide 12*).
5. $\pi\pi$ spectrum unfolded → **cross section in $\sqrt{\boldsymbol{s'}}$**, blinded contribution to a_μ computed to first check uncertainties.
6. After approval from the collaboration, $\pi\pi$ cross section and **contribution to $\boldsymbol{a_\mu}$** are **unblinded** (*slides 13-14*).

2-dimensional selection against background

Next-to-leading-order **(NLO) ISR**

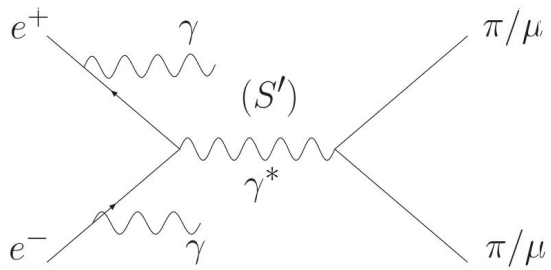

Next-to-leading-order **(NLO) FSR**

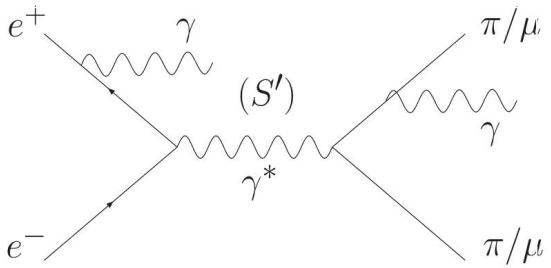

2 kinematic fits based on additional radiation:

→ small angle **(SA)** γ from beams

→ large angle **(LA)** γ from beams

Larger background in $\pi\pi\gamma$ process, suppressed with optimized BDT-based **2D-χ^2 selection** (98-99% signal efficiency).

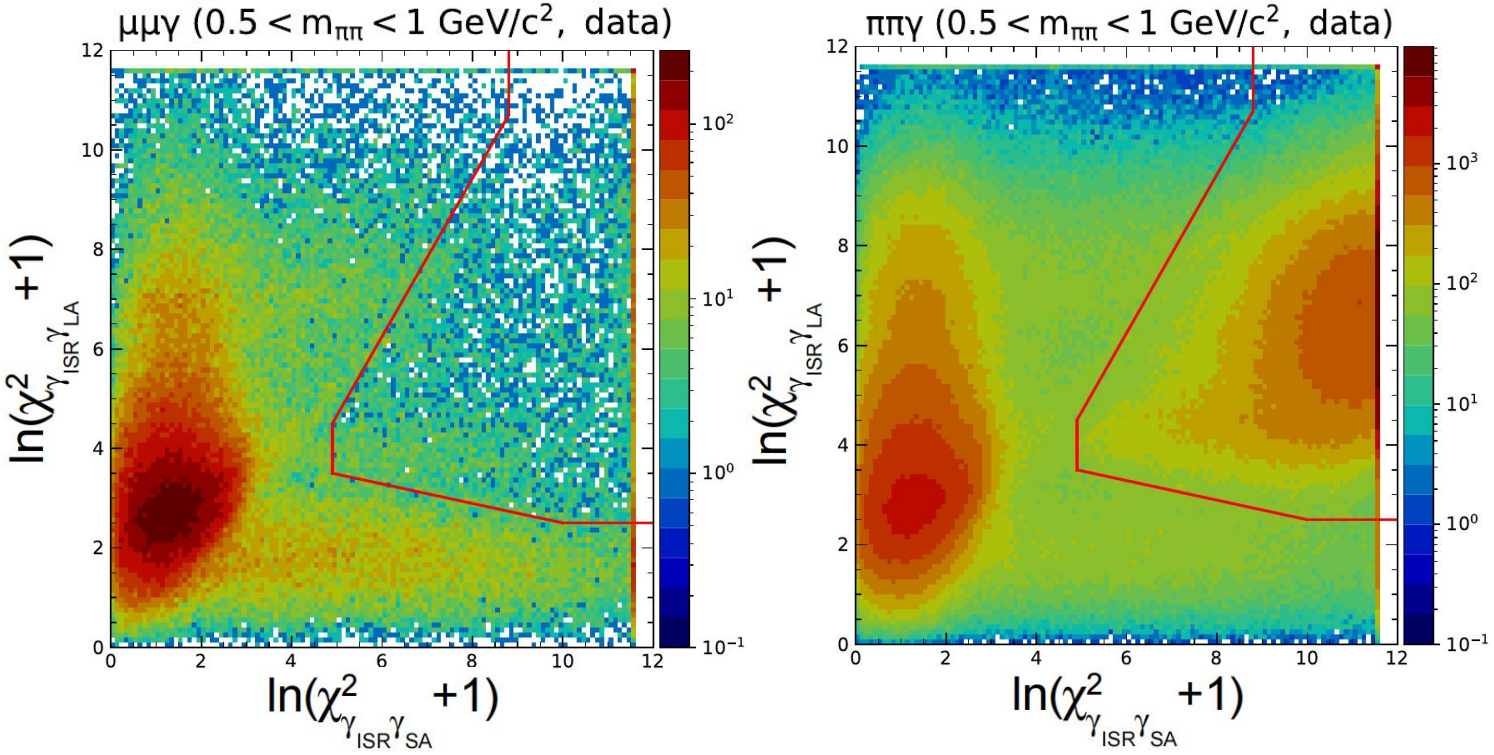

Methodology of the angular fits

$|\cos\theta^*|$ fits on background-subtracted data distributions with:

- templates of $\boldsymbol{\pi\pi\gamma}$, $\boldsymbol{\mu\mu\gamma}$ **and** $\boldsymbol{KK\gamma}$ obtained from MC simulation + small data/MC corrections studied separately,
- **data-driven** templates of $\boldsymbol{ee\gamma}$ process (no reliable simulation) using cut-based and BDT selections.

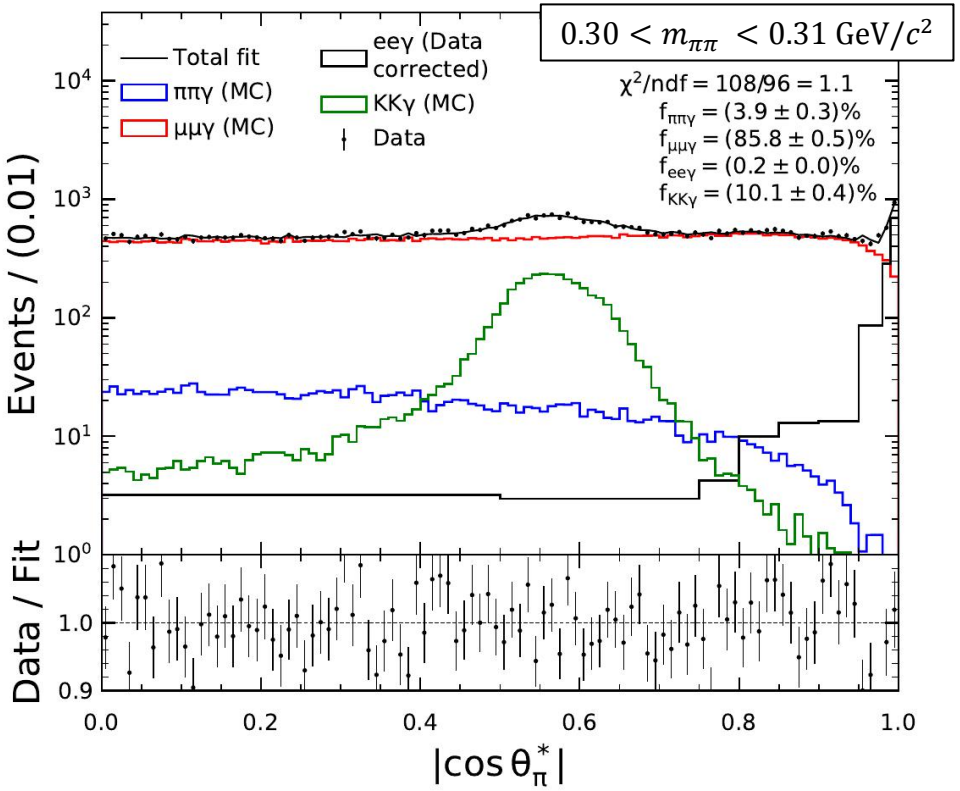

Fits in pion ($\boldsymbol{m_{\pi\pi}}$) and muon ($\boldsymbol{m_{\mu\mu}}$) mass hypotheses to get both $\pi\pi\gamma$ and $\mu\mu\gamma$ spectra in their respective basis.

→ linear combination of normalized templates in 2 MeV/c² mass bins between 0.5 - 1 GeV/c² (large $\pi\pi\gamma$ statistics), 10 MeV/c² elsewhere.

<u>3-step strategy for the fits</u>:

- **1st fit** in range $[0.9, 1]$ to get the $ee\gamma$ normalization,
- **2nd fit** in range $[0, 0.9]$ after subtracting $ee\gamma$ from data,
- $[0.9, 1]$ contribution **extrapolated** from 2nd fit result.

} **reduces sensitivity** to systematic errors on data-driven $ee\gamma$ determination.

⇒ **Closure test of accuracy** of the fit on simulation has shown that resulting spectra are **consistent with initial inputs**.

Corrections to simulation

Efficiency corrections determined for $|\cos\theta^*|$ templates and fitted masses due to data/MC differences, e.g. in 2D-χ^2 selection or trigger and tracking efficiencies (***corrections initially blinded***).

Large effect of corrections on mass spectra (at most ±5% difference to uncorrected spectra), however they tend to cancel when combined.

Overall, total template and mass corrections are rather flat (larger errors in ρ region from templates in muon mass).

$\mu\mu\gamma$ $\pi\pi\gamma$

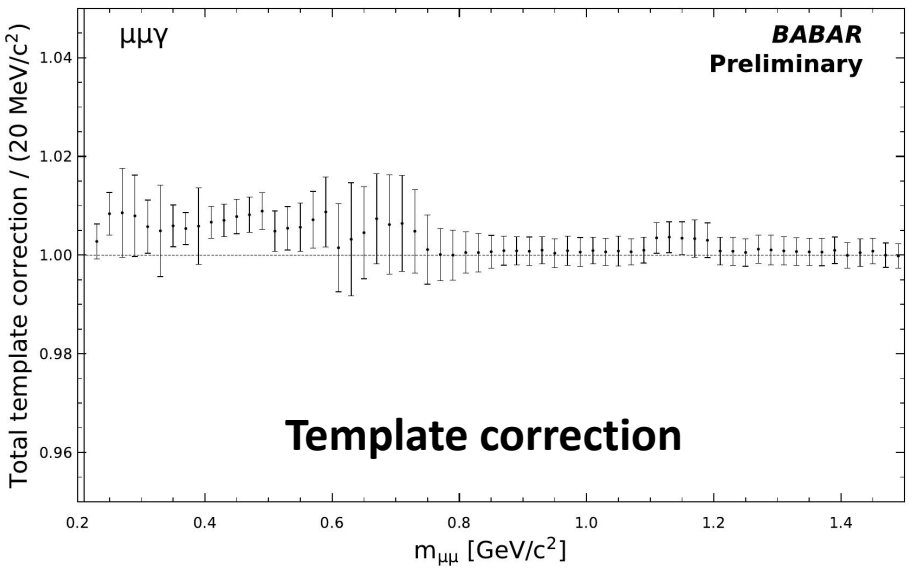

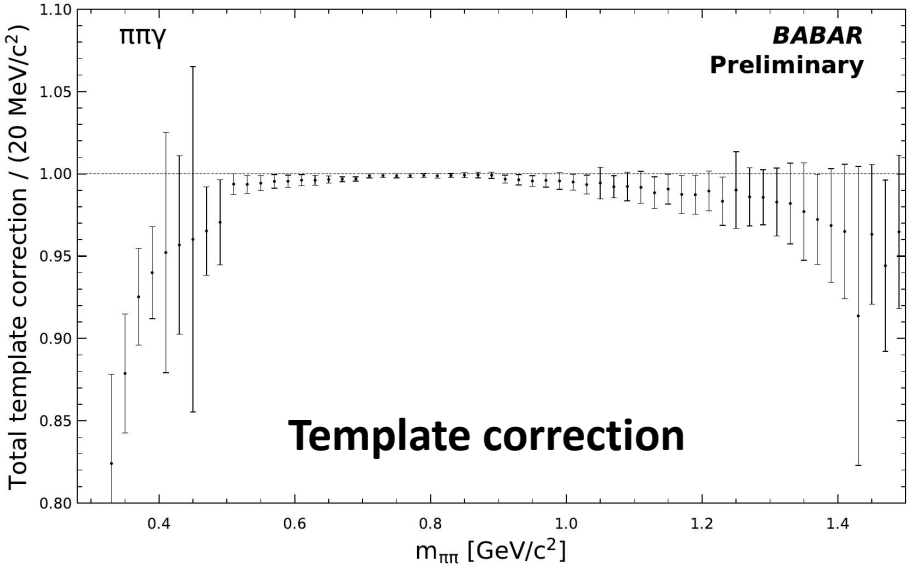

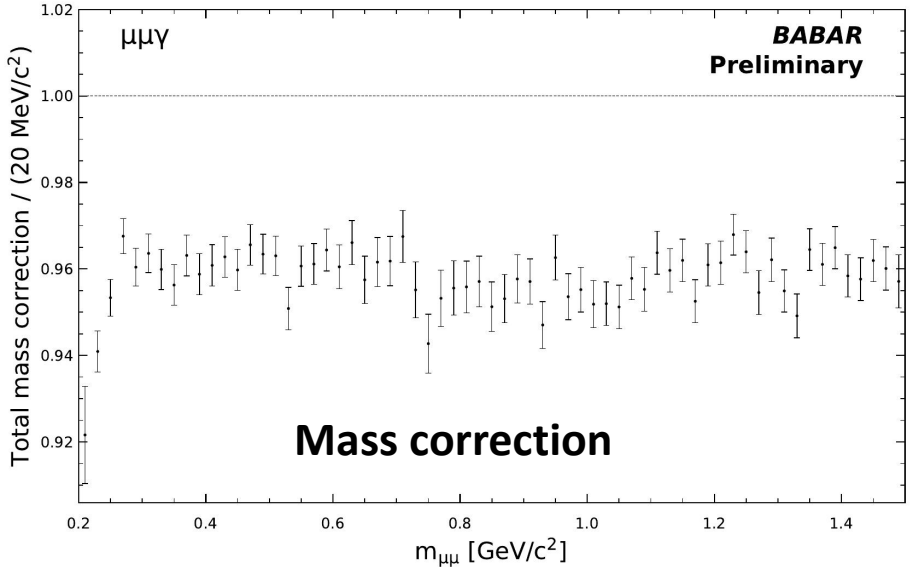

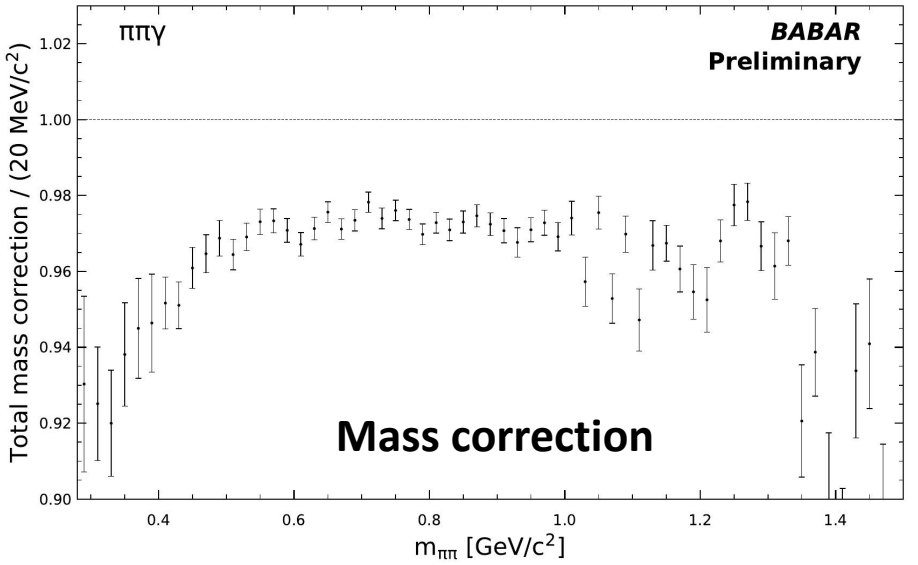

$\mu\mu\gamma$ & $\pi\pi\gamma$ mass spectra

Mass spectra obtained from angular fit with corrected templates.
Masses also corrected for mass-dependent efficiencies.

Normalization of each spectrum ***initially blinded*** with a multiplicative factor. Here shown after unblinding.

Statistical errors computed with bootstrap method.

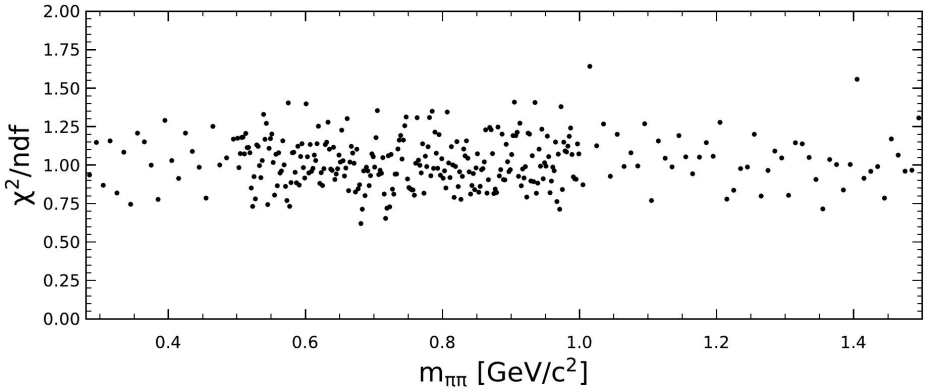

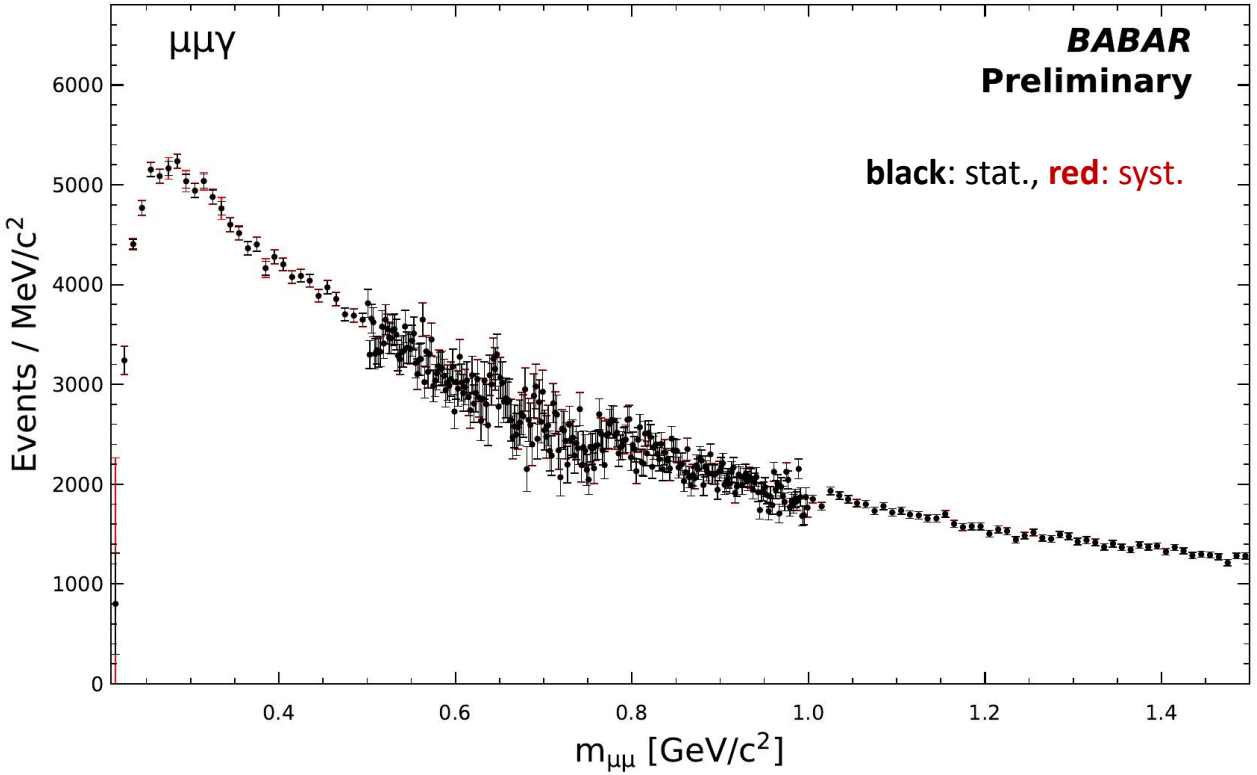

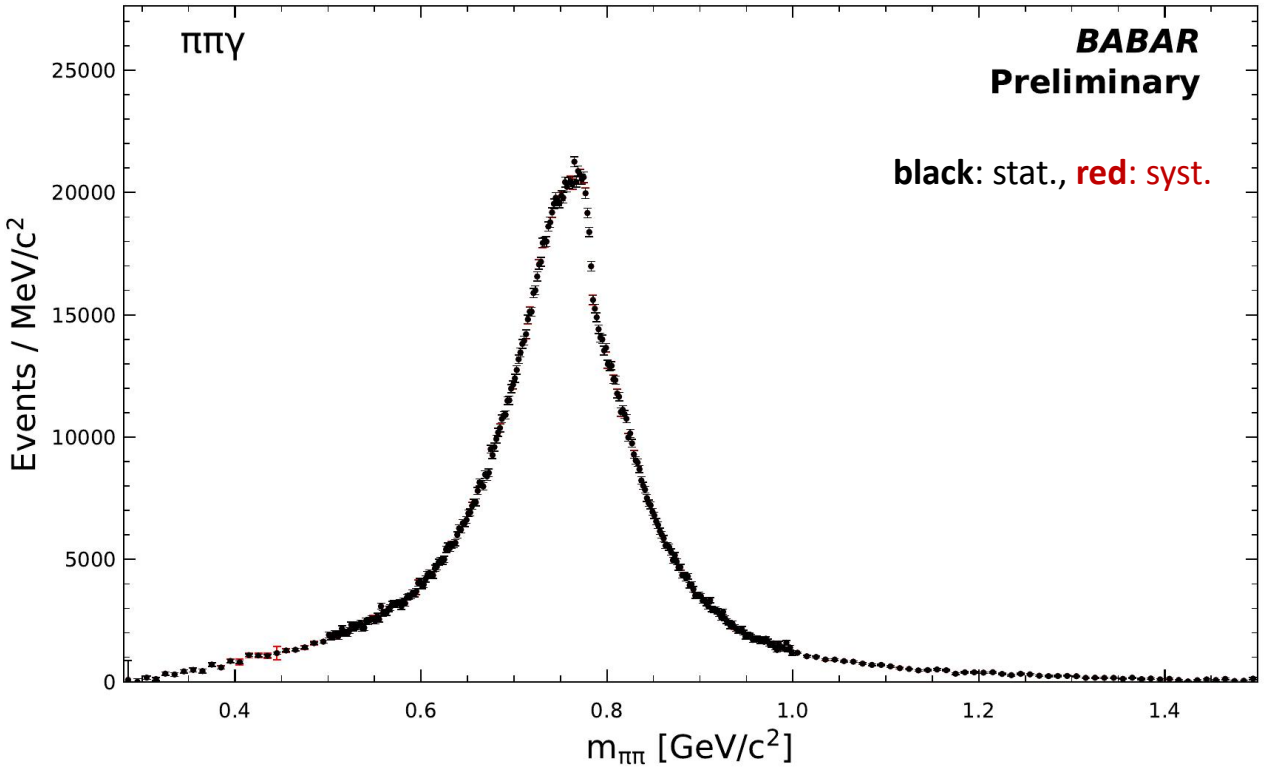

$\mu\mu\gamma$ spectrum comparison to QED prediction

$\mu\mu\gamma$ data spectrum can be **compared to QED prediction**, obtained from corrected simulated *Phokhara* spectrum.

The data/QED ratio is fitted with a constant:

$$0.9955 \pm \underbrace{0.0035_{\text{stat}}}_{\substack{\textit{data + stat}\\ \textit{errors on}\\ \textit{corrections}}} \pm \underbrace{0.0030_{\text{fit}}}_{\substack{\textit{syst errors on}\\ \textit{corrections}}}$$

(relevant only to this test)

$$\pm \underbrace{0.0033_{\gamma\ \text{ISR}}}_{\substack{\textit{ISR photon}\\ \textit{data/MC}\\ \textit{efficiency}}} \pm \underbrace{0.0043_{\text{lumi}\ ee}}_{\substack{\textit{error on}\\ e^+e^-\\ \textit{luminosity}}}$$

compatible with unity within a precision of 0.71%
⇒ **validates the $\pi\pi/\mu\mu$ separation procedure.**

**** includes systematics + correlations***

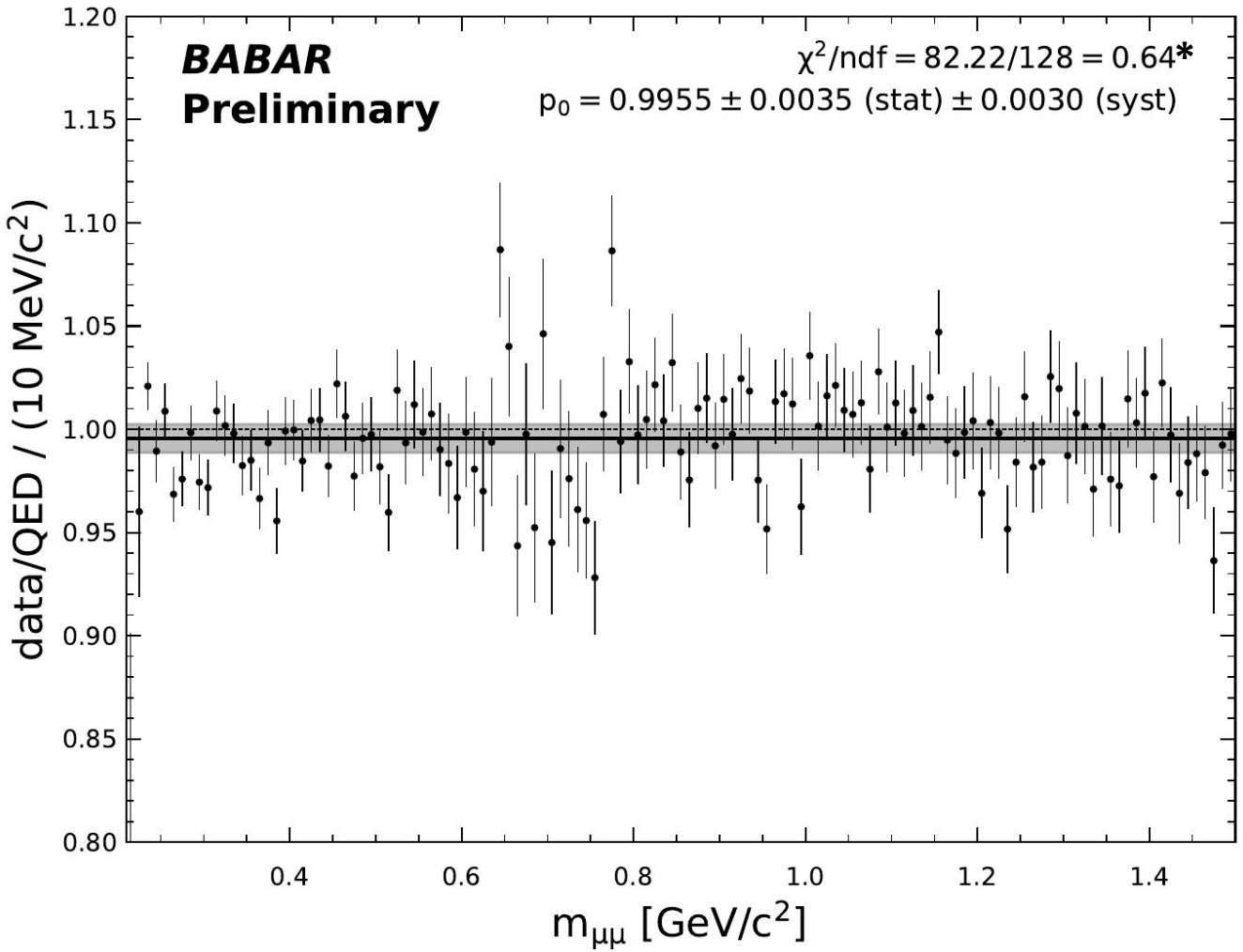

Determination of the ISR luminosity

Effective ISR luminosity obtained from unfolded $\mu\mu\gamma$ data spectrum $dN_{\mu\mu}^{\mathrm{ISR}}/d\sqrt{s'}$:

$$\frac{dL_{\mathrm{ISR}}^{\mathrm{eff}}}{d\sqrt{s'}} = \frac{dN_{\mu\mu}^{\mathrm{ISR}}/d\sqrt{s'}}{\epsilon_{\mu\mu}(\sqrt{s'})\,\sigma_{\mu\mu}^{0}(\sqrt{s'})}$$

mitigate statistical fluctuations

$$\underbrace{\frac{dN_{\mu\mu}^{\mathrm{MC\ gen}}}{d\sqrt{s'}}}_{\text{Phokhara spectrum at generation level}} \times \underbrace{(1 - f_{\mathrm{LO\ FSR}})}_{\text{removes the LO FSR contribution}} \times \underbrace{f_{\mu\mu}(\sqrt{s'})}_{\text{2nd order polynomial fit to data/MC}}$$

where $\epsilon_{\mu\mu}$ = acceptance of the selection (total efficiency) for muons,

$\sigma_{\mu\mu}^{0}$ = $\mu\mu$ bare cross section without vacuum polarization (VP).

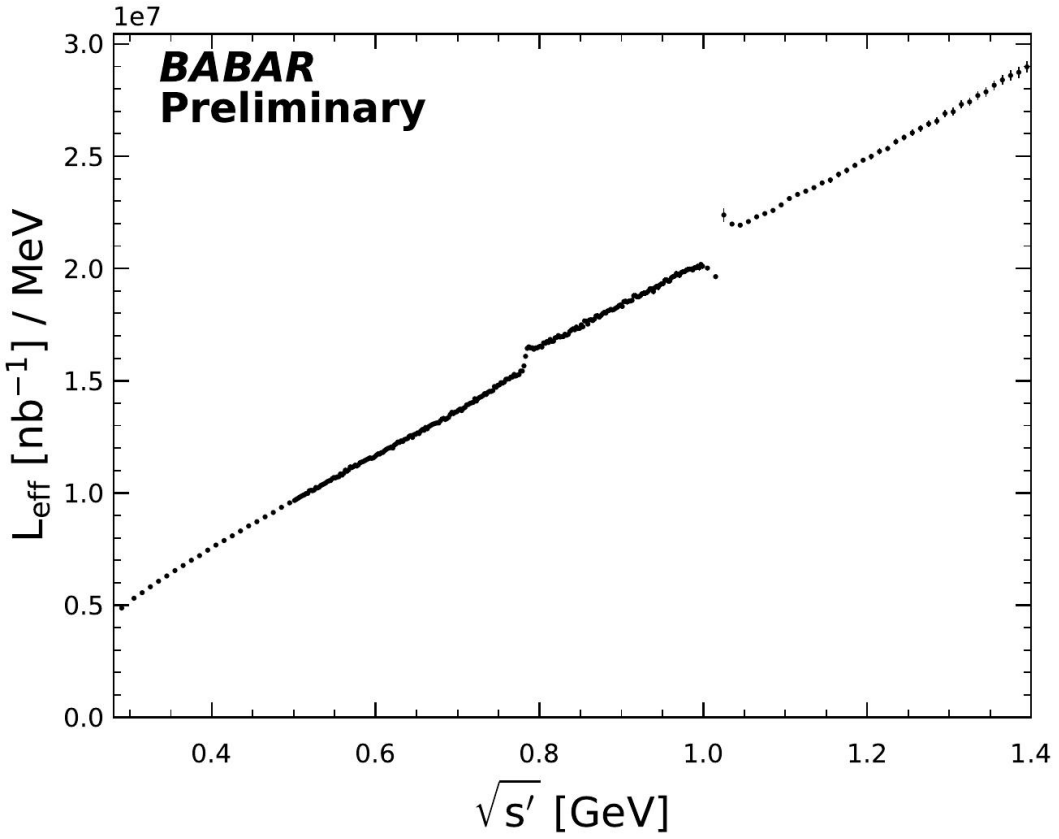

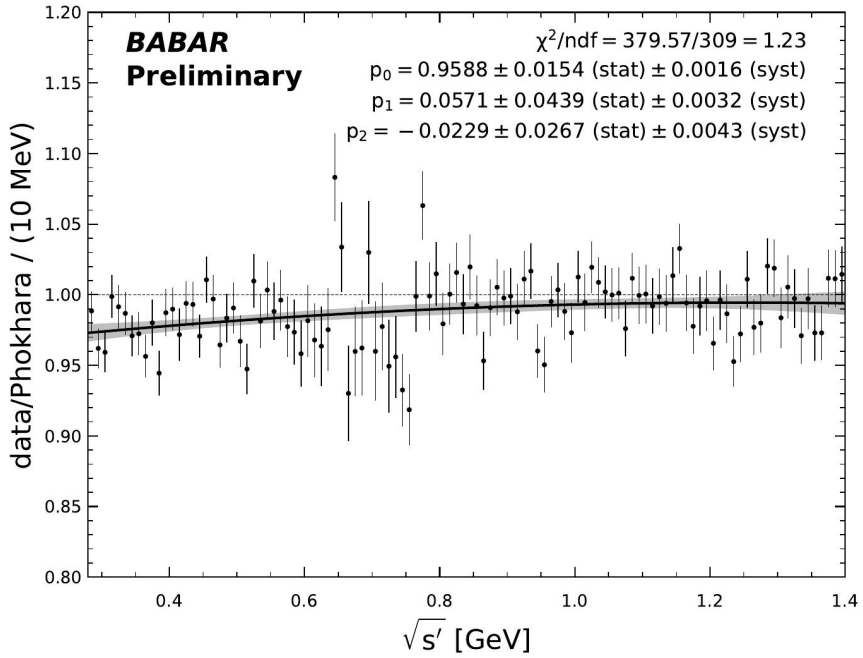

Measurement of the $e^+e^- \to \pi^+\pi^-(\gamma)\gamma_{\rm ISR}$ cross section

Bare cross section for the $\pi\pi$ process obtained from unfolded data spectrum using:

$$\sigma^0_{\pi\pi}(\sqrt{s'}) = \frac{dN_{\pi\pi}/d\sqrt{s'}}{\epsilon_{\pi\pi}(\sqrt{s'})\ dL^{\rm eff}_{\rm ISR}/d\sqrt{s'}}$$

where $\epsilon_{\pi\pi}(\sqrt{s'})$ = acceptance of the selection (total efficiency) for pions.

⇒ equivalent to: $$\sigma^0_{\pi\pi}(\sqrt{s'}) = \sigma^0_{\mu\mu}(\sqrt{s'}) \frac{dN_{\pi\pi}/d\sqrt{s'}}{dN^{\rm MC\ gen}_{\mu\mu}/d\sqrt{s'}} \frac{1}{(1-f_{\rm LO\ FSR})\ f_{\mu\mu}(\sqrt{s'})} \frac{1}{\epsilon_{\pi\pi}(\sqrt{s'})}$$

⇒ ensures cancellation of common $\pi\pi/\mu\mu$ systematic effects (e^+e^- luminosity, ISR photon efficiency, VP...).

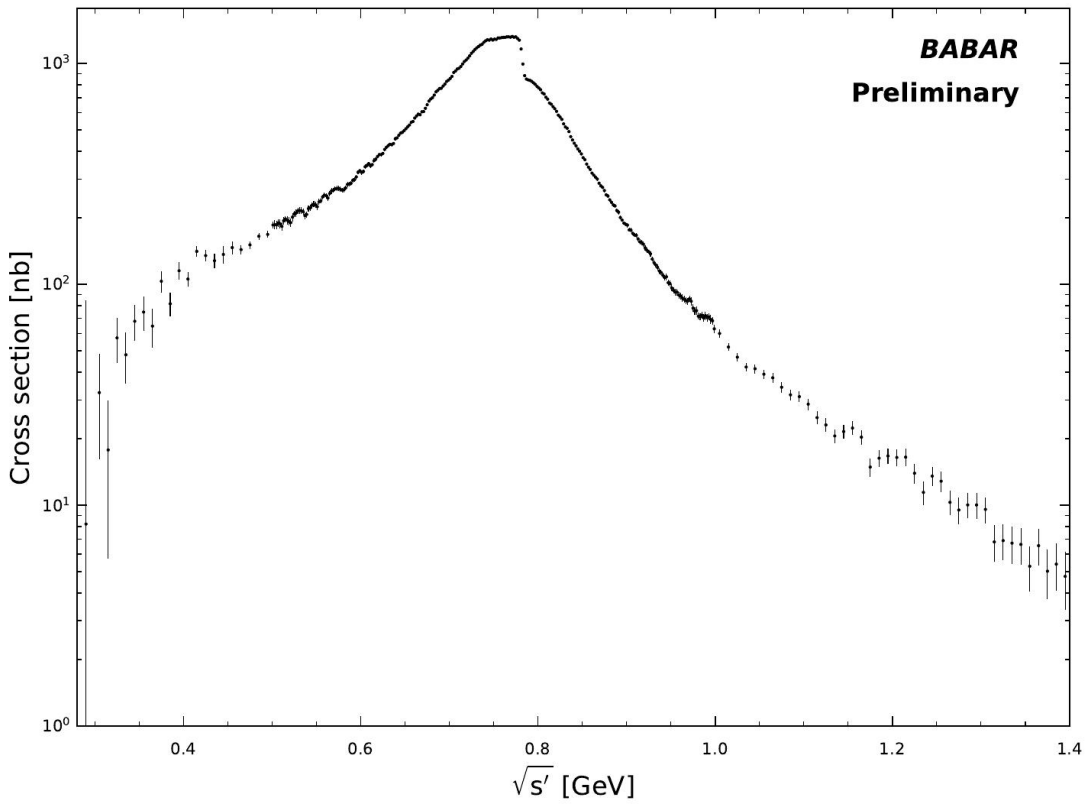

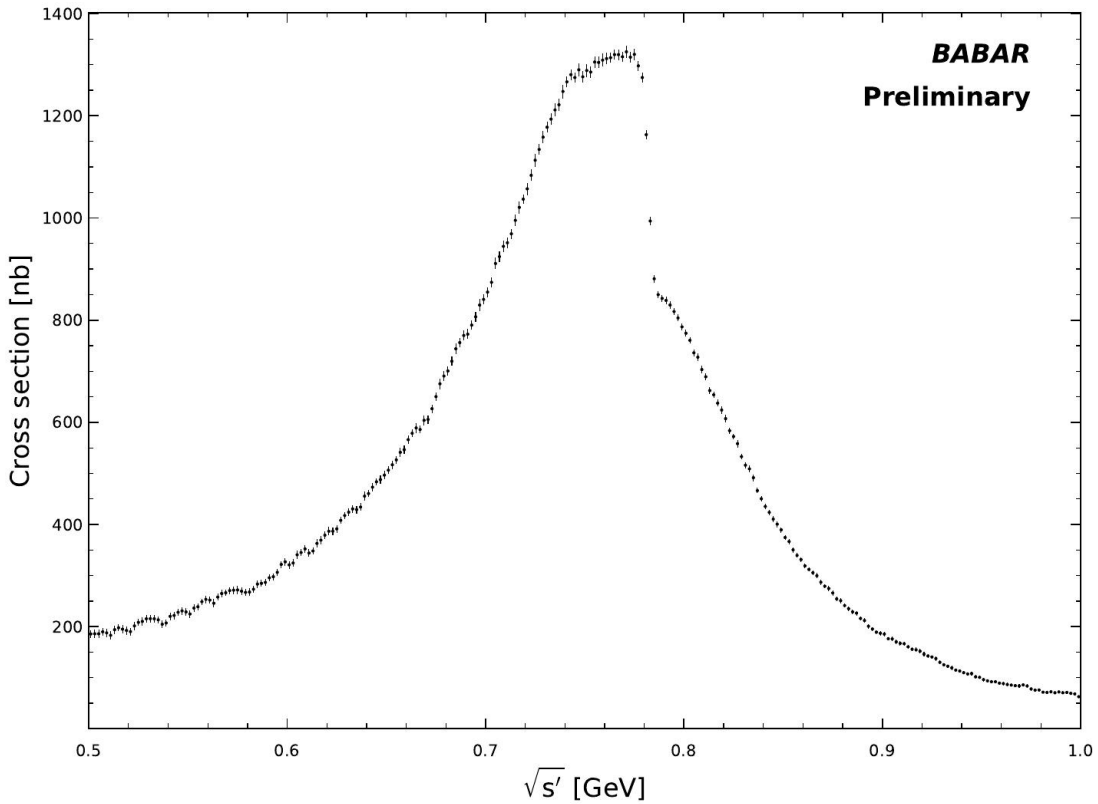

$\pi\pi$ contribution to a_μ and comparison to 2009 result

The 2025 cross section looks overall in good agreement with the previous measurement from 2009, except at large energies.

Not competitive at low/high energies because muons dominate this region: poor precision on the determination of pion fraction in the angular fit.

$\pi\pi$ contributions to a_μ

Energy range [GeV]	2025 $a_\mu^{2\pi}$ ± stat ± syst [10^{-10}]	2009 $a_\mu^{2\pi}$ ± stat ± syst [10^{-10}]
Below 0.5	58.0 ± 5.5 ± 1.7	58.2 ± 0.6 ± 0.6
0.5 - 1.4	456.2 ± 2.2 ± 1.7	455.6 ± 2.1 ± 2.6

Energy range [GeV]	2025-2009 average (preliminary) $a_\mu^{2\pi}$ [10^{-10}]
Below 0.5	58.2 ± 0.8
0.5 - 1.4	455.9 ± 2.1
Below 1.4	514.1 ± 2.5
Below 1.8 (1.4 - 1.8 from 2009)	514.4 ± 2.5

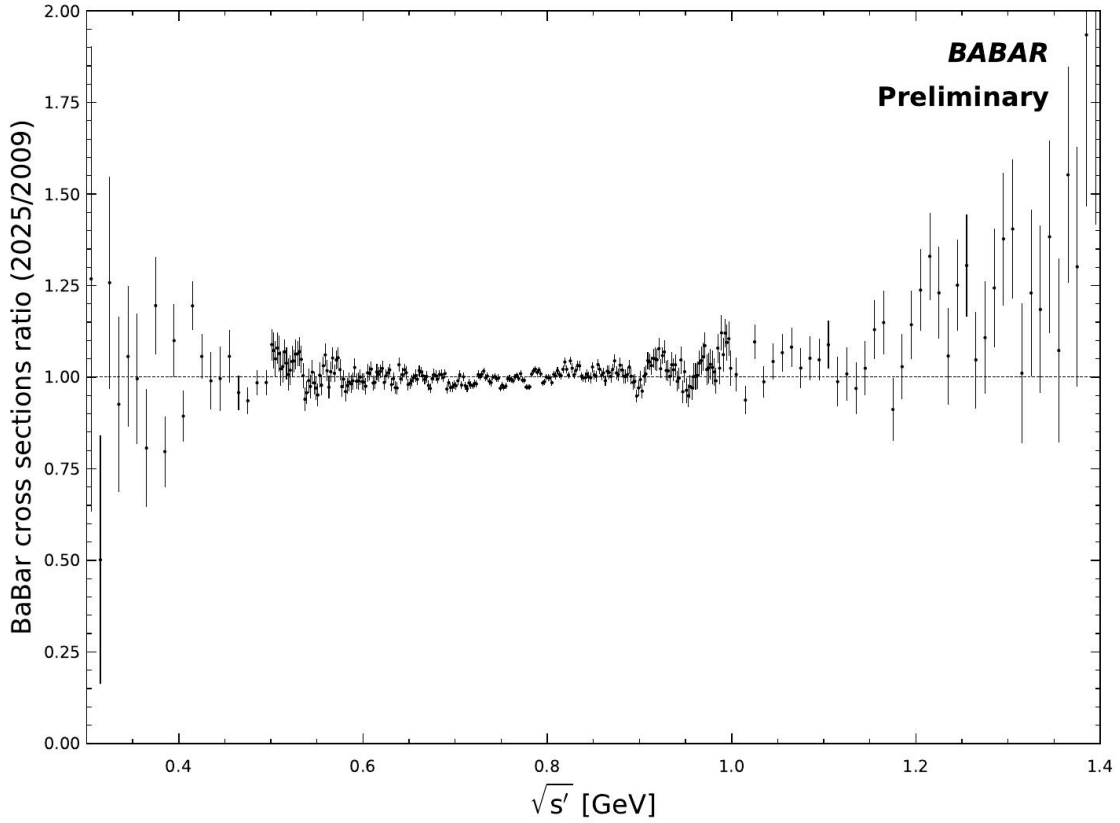

⇒ **2025 and 2009 results are compatible with excellent agreement**

⇒ **the averages yield the most precise $a_\mu^{2\pi}$ measurement from a single experiment.**

Summary and conclusion

- Contribution of $\pi\pi$ channel to a_μ measured by BaBar via ISR in a new blinded analysis, following an independent method from the previous 2009 measurement with full data statistics of around 460 fb^{-1}.
- Separation of $\pi\pi$ and $\mu\mu$ final states in data carried out with fits of angular distributions.
  PID requirements removed in this work (dominant systematics in the 2009 study).
- Unblinded $\mu\mu\gamma$ spectrum compared to QED prediction, showing compatibility with unity within uncertainties.
- Unblinded $\pi\pi$ cross section found to be in good agreement with the 2009 measurement, leading to the values of

$$a_\mu^{2\pi,\,2025} = \left(58.0 \pm 5.5\,(\text{stat}) \pm 1.7\,(\text{syst})\right) \times 10^{-10}$$ *below 0.5 GeV,*

$$a_\mu^{2\pi,\,2025} = \left(456.2 \pm 2.2\,(\text{stat}) \pm 1.7\,(\text{syst})\right) \times 10^{-10}$$ *between 0.5 - 1.4 GeV,*

  both very close to the previous 2009 results. Comparable statistical errors and reduced systematics between 0.5 - 1.4 GeV (*still preliminary*).

⇒ This consistency obtained with an independent and fully blinded procedure shows the robustness of both analyses, which combined provide the most precise measurement of $a_\mu^{2\pi}$ from a single experiment.

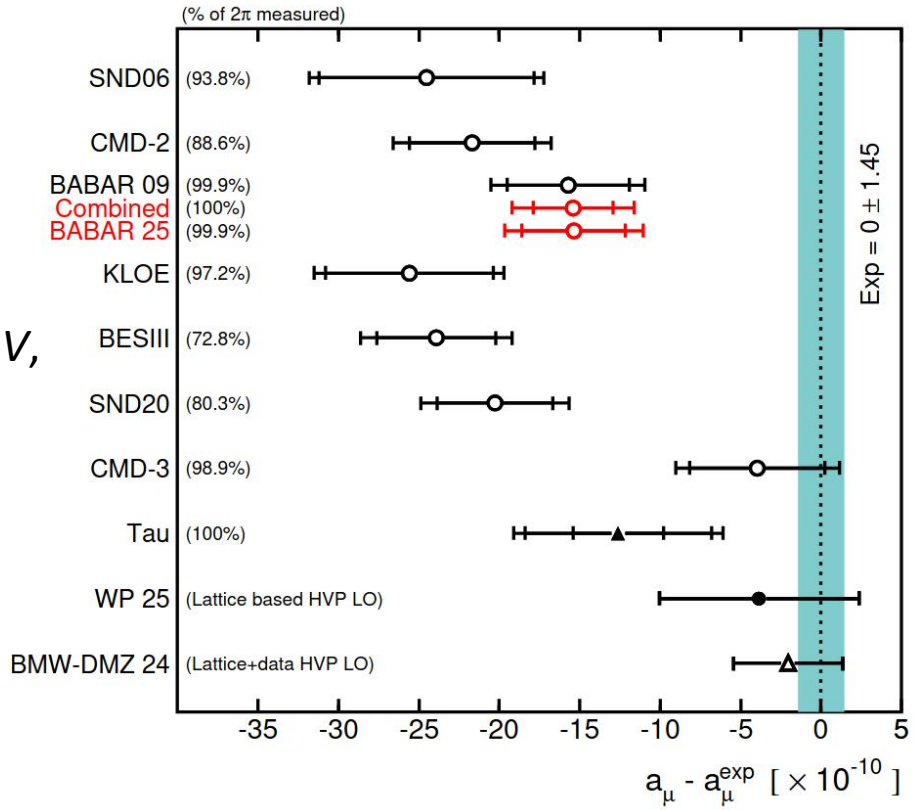

Backup

From $e^+e^- \to \pi^+\pi^-(\gamma)$ cross section to a_μ

Cross section of $e^+e^- \to X$ at **reduced energy** $\sqrt{s'} = m_X$ (X = any final state) from measurement of $e^+e^- \to X\gamma_{\mathrm{ISR}}$:

$$s' = s\left(1 - 2E^*_{\gamma_{\mathrm{ISR}}}/\sqrt{s}\right),$$

$E^*_{\gamma_{\mathrm{ISR}}} = \gamma_{\mathrm{ISR}}$ energy in center of mass (CM) frame.

Measuring the yield $N_{X\gamma_{\mathrm{ISR}}}$ gives the **bare cross section $\sigma^0_X(\sqrt{s'})$ (excluding vacuum polarization)**:

$$\frac{dN_{X\gamma_{\mathrm{ISR}}}}{d\sqrt{s'}} = \frac{dL^{eff}_{\mathrm{ISR}}}{d\sqrt{s'}}\ \varepsilon_{X\gamma_{\mathrm{ISR}}}(\sqrt{s'})\ \sigma^0_X(\sqrt{s'}) \qquad (1)$$

- $\varepsilon_{X\gamma_{\mathrm{ISR}}}$ = detection efficiency in acceptance → from simulation with data corrections.
- L^{eff}_{ISR} = effective ISR luminosity → from $X = \mu\mu(\gamma_{\mathrm{FSR}})$ in (1) and σ^0_X taken from QED computation.

Ratio of $\pi\pi$ and $\mu\mu$ mass spectra ⇒ cancellation of VP ⇒ ratio of (1) =

$$\frac{\sigma^0_{\pi\pi(\gamma_{\mathrm{FSR}})}(\sqrt{s'})}{\sigma_{\mathrm{pt}}(\sqrt{s'})(1+\delta^{\mu\mu}_{\mathrm{FSR}})(1+\delta^{\mu\mu}_{\mathrm{add.\ FSR}})}$$

- $\sigma_{\mathrm{pt}} = 4\pi\alpha^2/3s'$ = cross section for pointlike charged fermions.
- $(1+\delta^{\mu\mu}_{(\mathrm{add.})\ \mathrm{FSR}})$ = corrections for lowest-order (additional) FSR contributions.

Dispersion relation:

$$a_\mu^{\pi\pi(\gamma_{\mathrm{FSR}}),\ \mathrm{LO}} = \frac{1}{4\pi^3}\int_{4m_\pi^2}^{\infty} ds'\ K(s')\ \sigma^0_{\pi\pi(\gamma_{\mathrm{FSR}})}(s')$$

where $K(s')$ is a QED kernel, relates the bare cross section to the lowest-order contribution of $\pi\pi(\gamma_{\mathrm{FSR}})$ to a_μ.

$$K(s) = x^2\left(1-\frac{x^2}{2}\right) + (1+x)^2\left(1+\frac{1}{x^2}\right)\left[\ln(1+x) - x + \frac{x^2}{2}\right] + x^2\ln x\frac{1+x}{1-x},\ \ x = (1-\beta_\mu)(1+\beta_\mu),\ \ \beta_\mu = \text{muon velocity.}$$

NLO & NNLO fits description

- $\gamma_{\mathrm{ISR}}\gamma_{\mathrm{LA}}$ **fit**: additional **large angle (LA)** γ $(0.35 - 2.45$ rad) in EMC (threshold: energy > 50 MeV). Measured energy/angle of γ_{LA} used in fit.
- $\gamma_{\mathrm{ISR}}\gamma_{\mathrm{SA}}$ **fit**: additional **small angle (SA)** γ. No measured information: γ_{SA} assumed collinear with one of the beams. Additional photons in EMC ignored.

4-momentum conservation: use measured ISR energy/direction + momenta/angles of both tracks. Tracks assumed to be pions: similar to cross section measurement analysis.

Asymmetry of EMC response when $E_\gamma < E_{\mathrm{true}}$: ISR photon energy transformed to symmetric (gaussian) with Novosibirsk function $\rightarrow$ Z variable (3 parameters), initialized with measured E_γ.

χ^2 minimized according to 4-momentum conservation in terms of Z variable(s). Fitted energy obtained from returned Z values.

Same process in NNLO fits.

Angular fit: $\cos\theta^*_\pi$ or $|\cos\theta^*_\pi|$?

Asymmetry measured on $\cos\theta^*_\pi$ distributions:

$$\frac{H(\cos\theta^*_\pi > 0) - H(\cos\theta^*_\pi < 0)}{H(\cos\theta^*_\pi > 0) + H(\cos\theta^*_\pi < 0)}, H = \text{histogram}.$$

Linear regression along the $\cos\theta^*_\pi$ range to obtain a representative value in each $m_{\pi\pi}$ bin.

No significant asymmetry except for $\mu\mu\gamma$ (> 1 GeV/c^2): forward-backward asymmetry due to ISR-FSR interference.

→ **Fits performed on $|\cos\theta^*_\pi|$.**

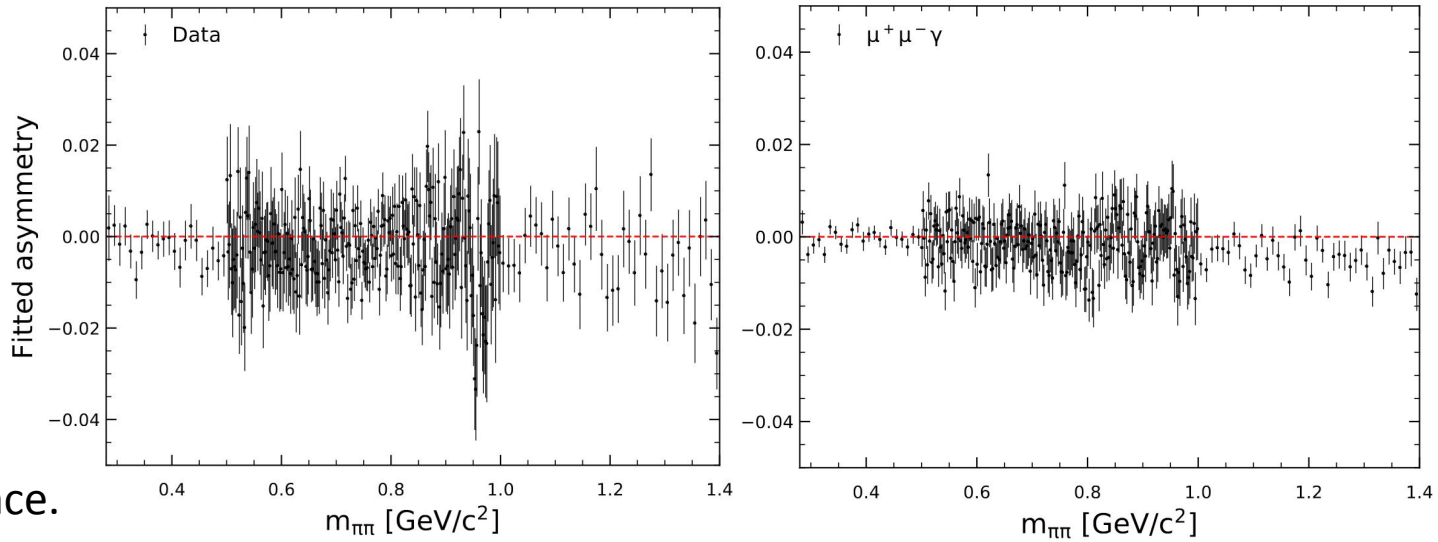

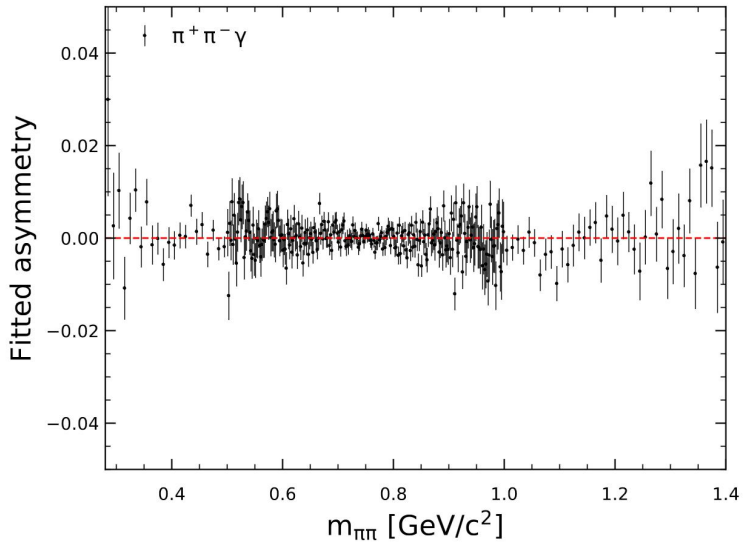

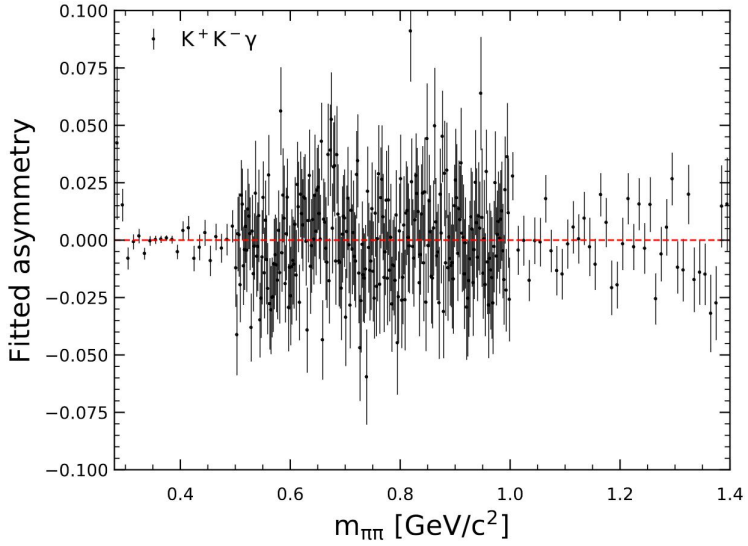

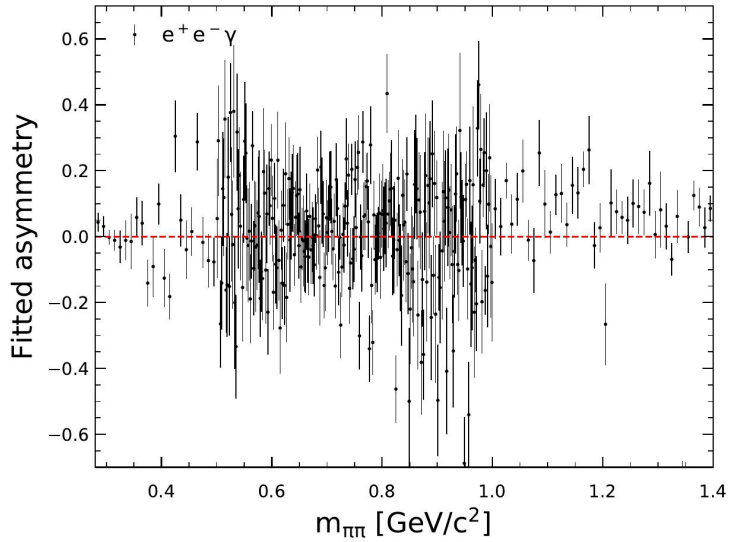

2D-χ^2 distributions (central mass region)

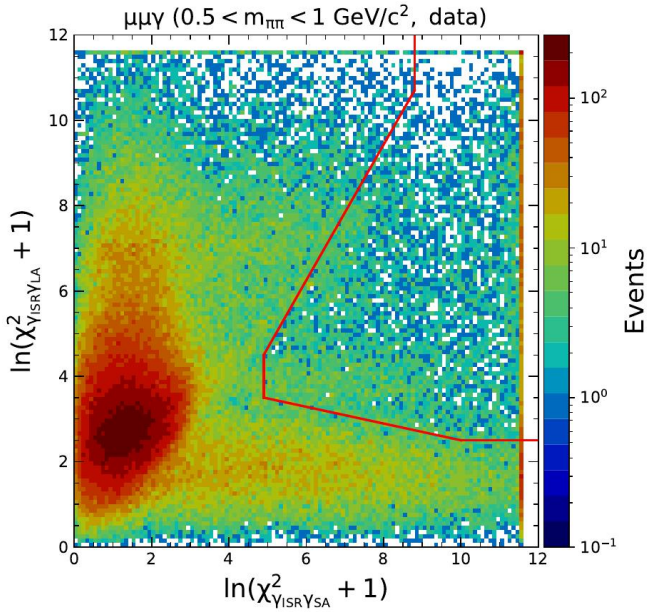

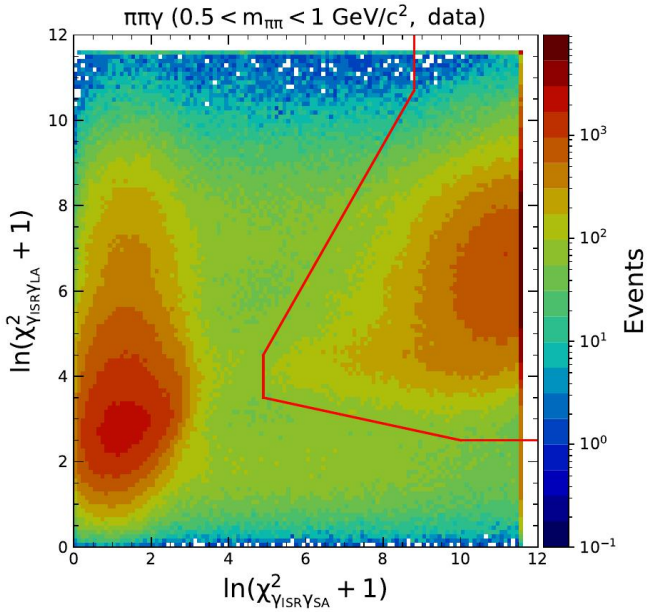

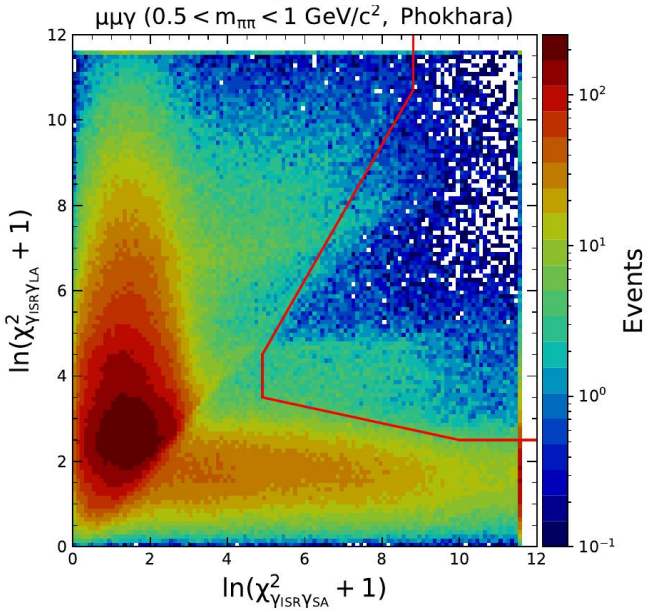

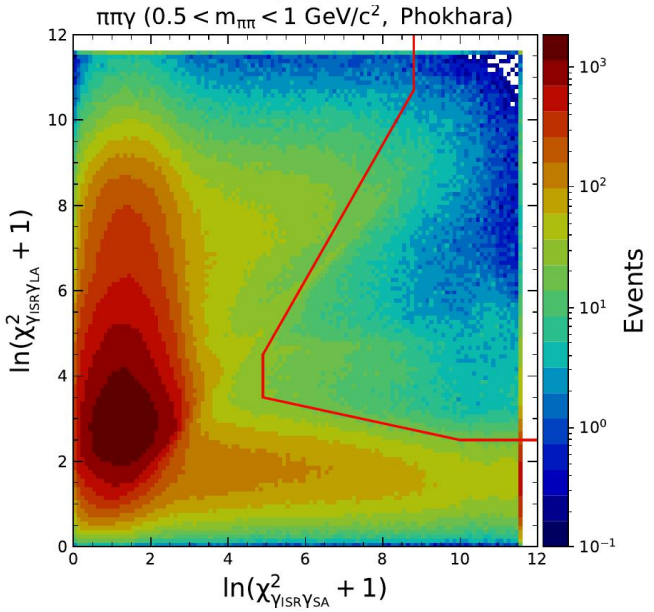

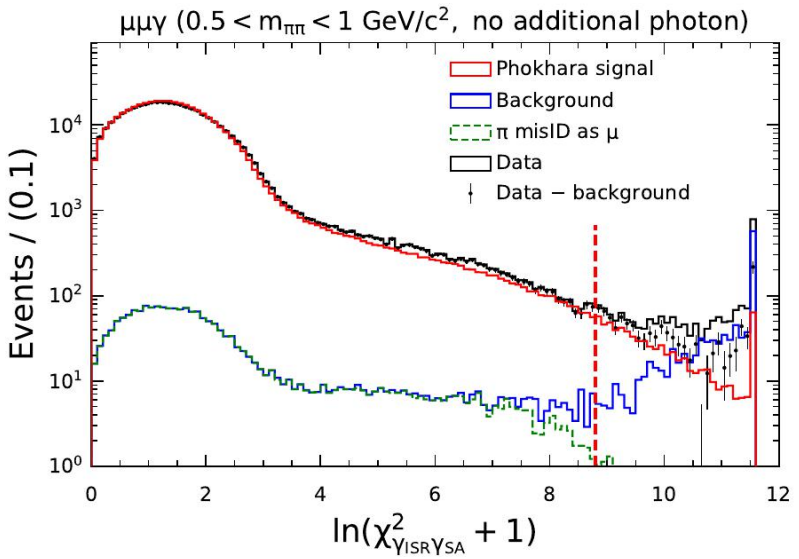

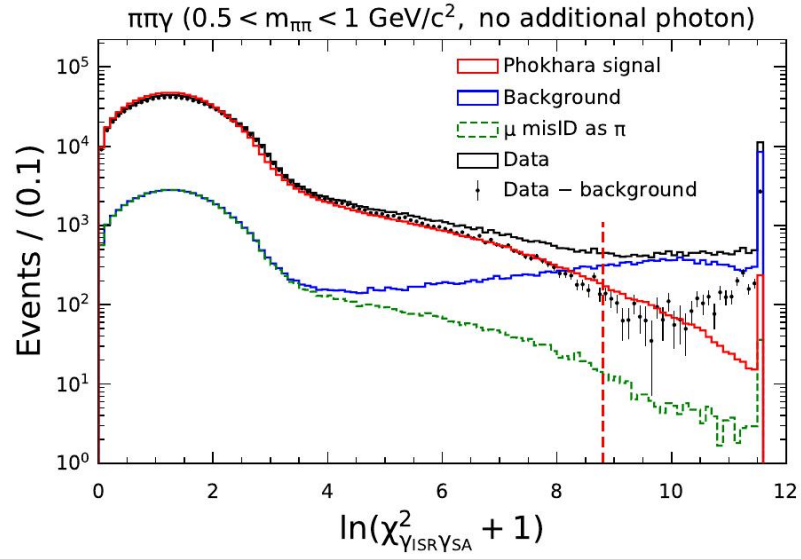

Cut-based selection of $ee\gamma$ events

Cut-based selection defined from a previous analysis (2015):

$$\left(\frac{E_{\text{cal}}}{p}\right)_1 > 0.5, \quad \left(\frac{dE}{dx}\right)_1 > 600,$$

$$\left(\frac{dE}{dx}\right)_2 > 550 + 60 \times p_2 + 8.9 \times p_2^2 ,$$

$$\text{isElectron}_{1/2} = \left(\frac{E_{\text{cal}}/p - 1}{0.15}\right)^2 + \left(\frac{dE/dx - 690}{150}\right)^2 < 10$$

where 1 (2) labels the track with the highest (lowest) momentum.

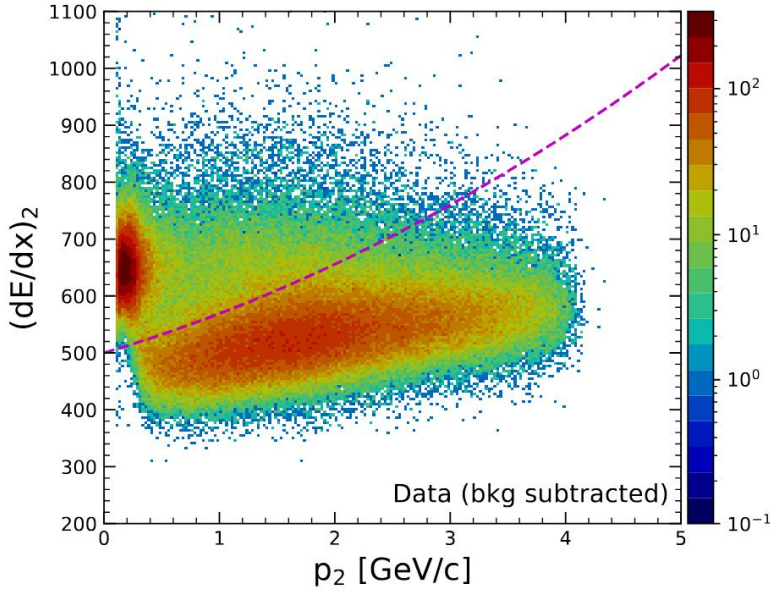

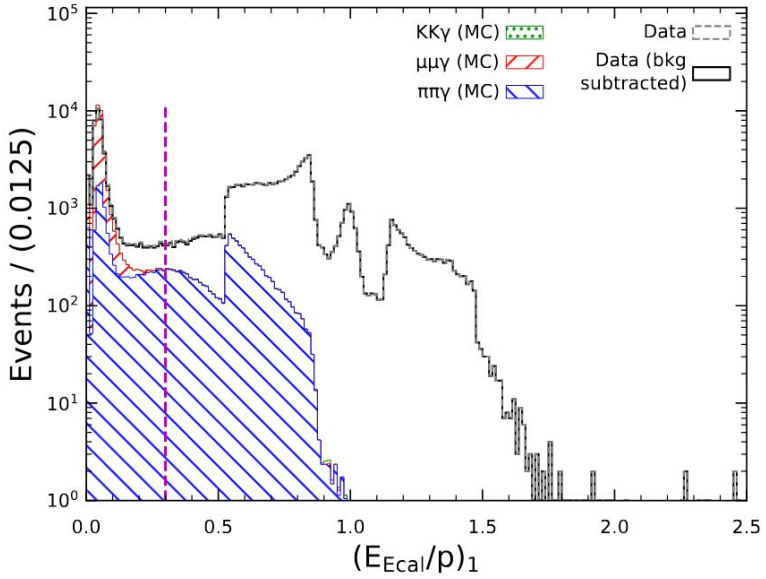

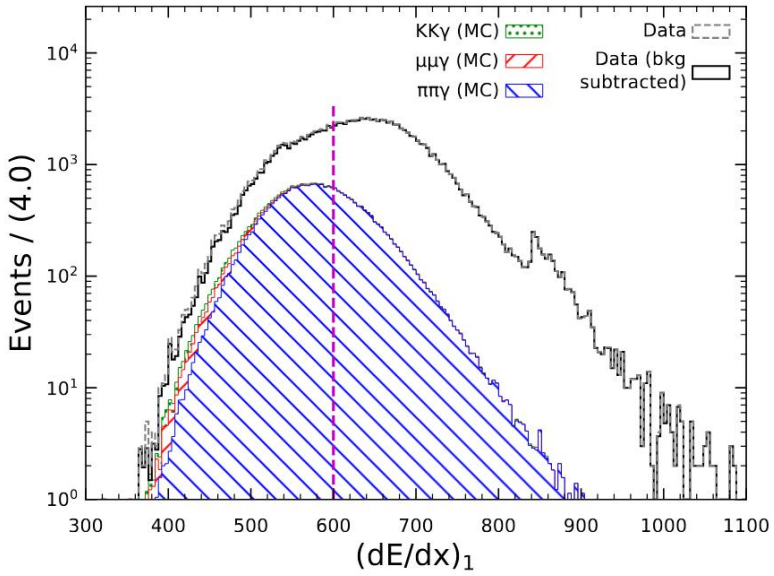

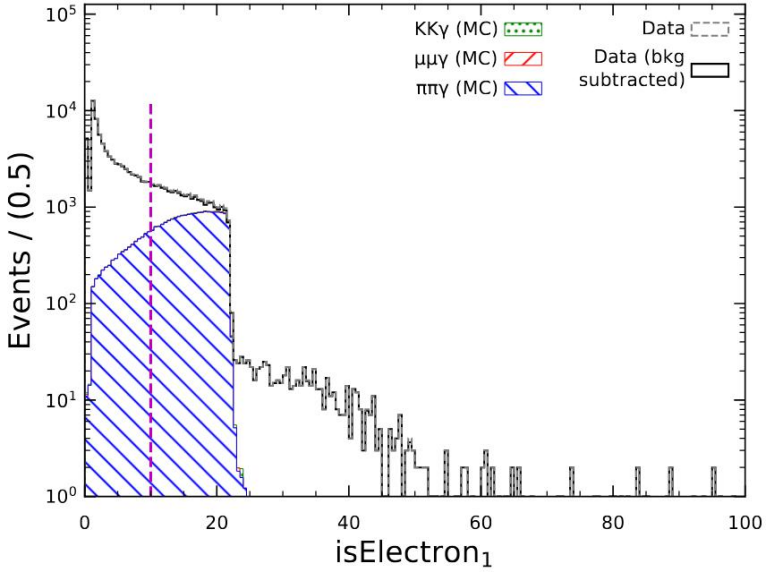

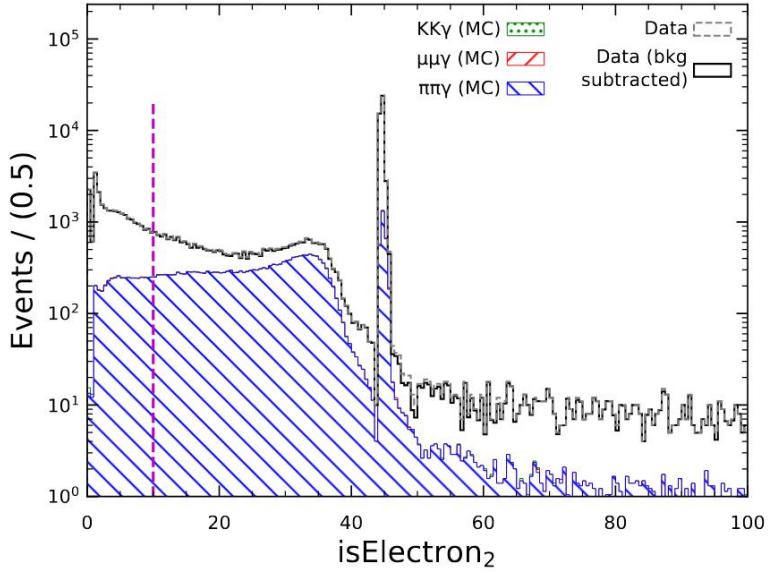

BDT-based selection of $ee\gamma$ events

Additional **selection based on a BDT** with XGBoost library, using variables:

$$(E_{\mathrm{Ecal}}/p)_1,\ (dE/dx)_{1/2},\ p_{1/2},\ \mathrm{isElectron}_{1/2},\ V_{xy},\ m_{\pi\pi},\ m_{\mu\mu}$$

Training on events passing the cut-based selection: data = signal, MC = background.

Parameters of BDT (depth of tree, learning rate...) optimised to improve accuracy.

Two BDTs trained on one half of the sample, applied to the other to avoid any bias.

Evaluation metric = logarithmic loss function, early stopping implemented to prevent overfitting in the training.

Output: probability for an event to be signal (i.e. $ee\gamma$-like).

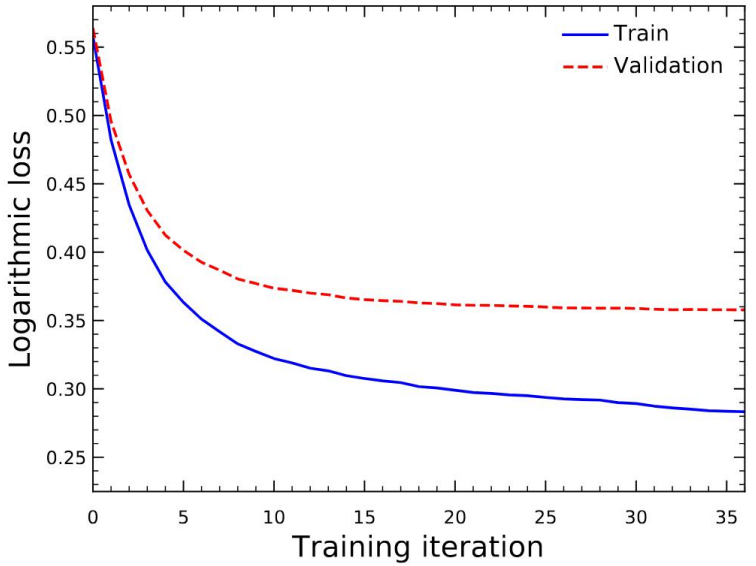

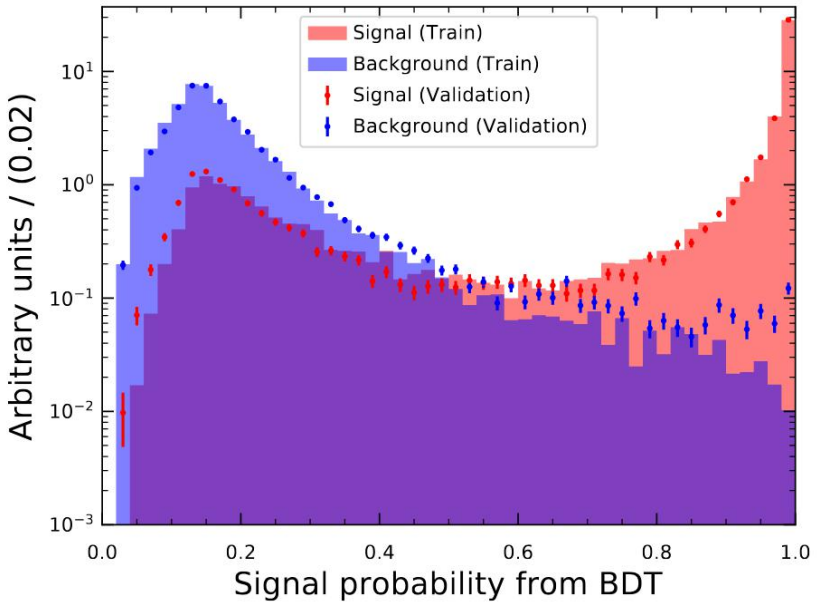

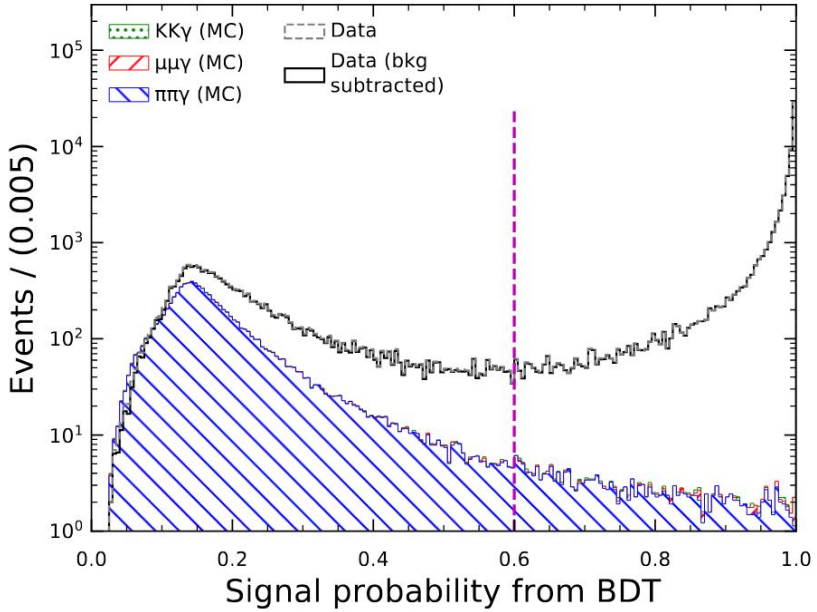

$\pi\pi\gamma$ background in $ee\gamma$ sample

Important background retained by both cut-based and BDT selections (mostly $\pi\pi\gamma$).

Data/MC comparison performed on $\pi\pi\gamma$ dominated sample → correct the background before subtraction from the $ee\gamma$ selected sample in data.

$\pi\pi\gamma$ sample selection:

$$(E_{Ecal})_1 > 0.5\ \text{GeV} \quad \& \quad (E_{Ecal})_2 > 0.3\ \text{GeV} \quad \& \quad 0.6 < m_{\pi\pi} < 0.9\ \text{GeV}/c^2 \quad \& \quad |\cos\theta^*_\pi| < 0.9$$

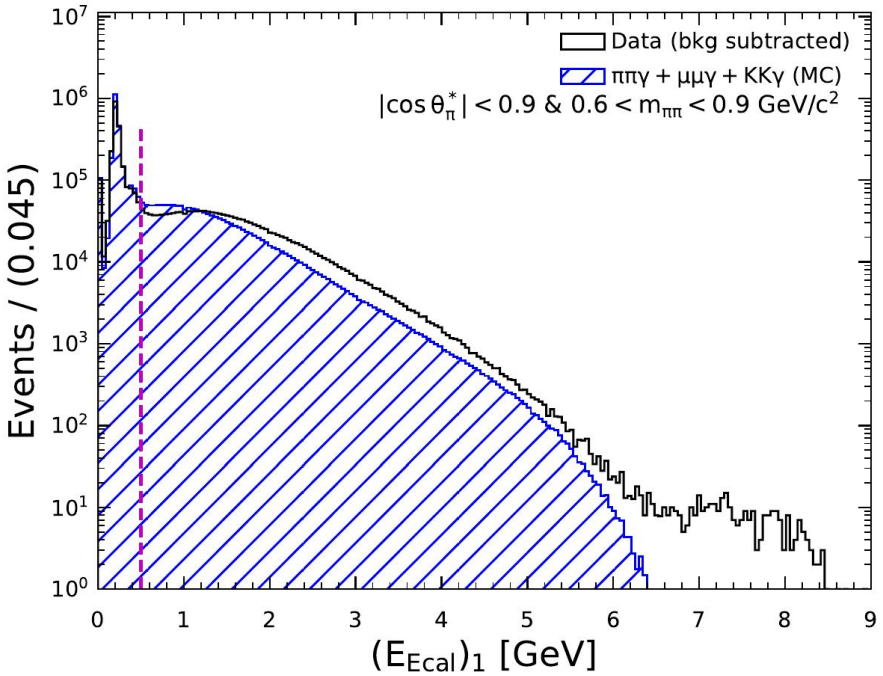

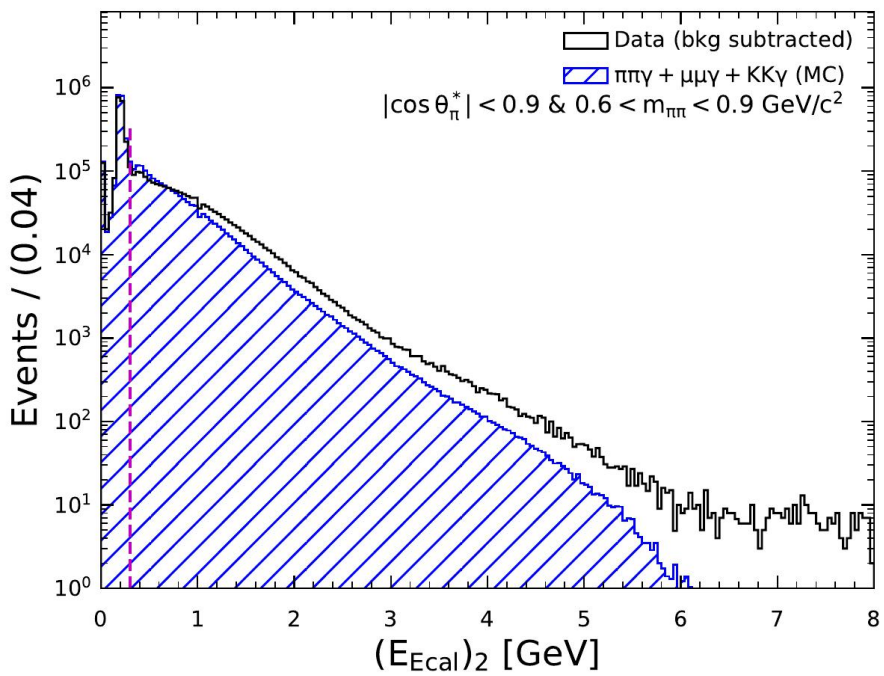

$\pi\pi\gamma$ background in $ee\gamma$ sample

Cuts effective in removing $\mu\mu\gamma$ events, also $ee\gamma$ but only between $0.7 - 0.85\ \mathrm{GeV}/c^2$.

Rate of $\pi\pi\gamma$ events that pass the $ee\gamma$ selection in data and MC compared by taking the ratio.

MC underestimates the $\pi\pi\gamma$ background retained by cut at 0.6 in the enriched sample

→ discrepancy mostly due to the cut $(E_{\mathrm{Ecal}}/p)_1 > 0.5$,

→ cuts on $(dE/dx)_{1/2}$ better reproduced.

Background scaling factor obtained by linear fit, fixed where statistics is missing.

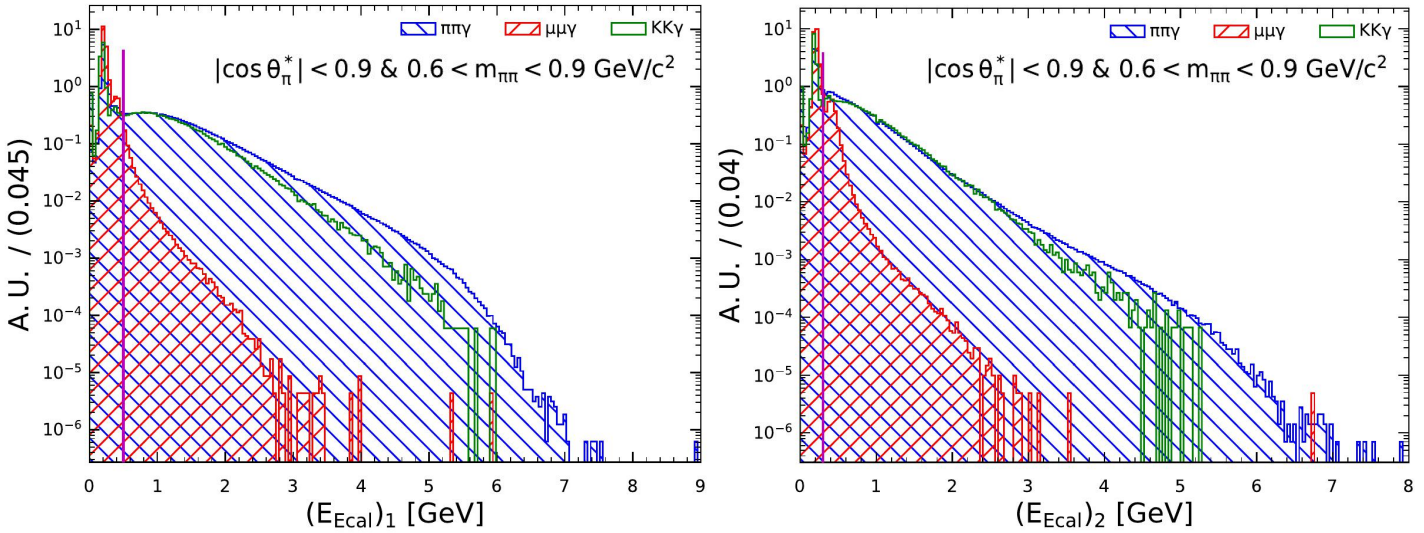

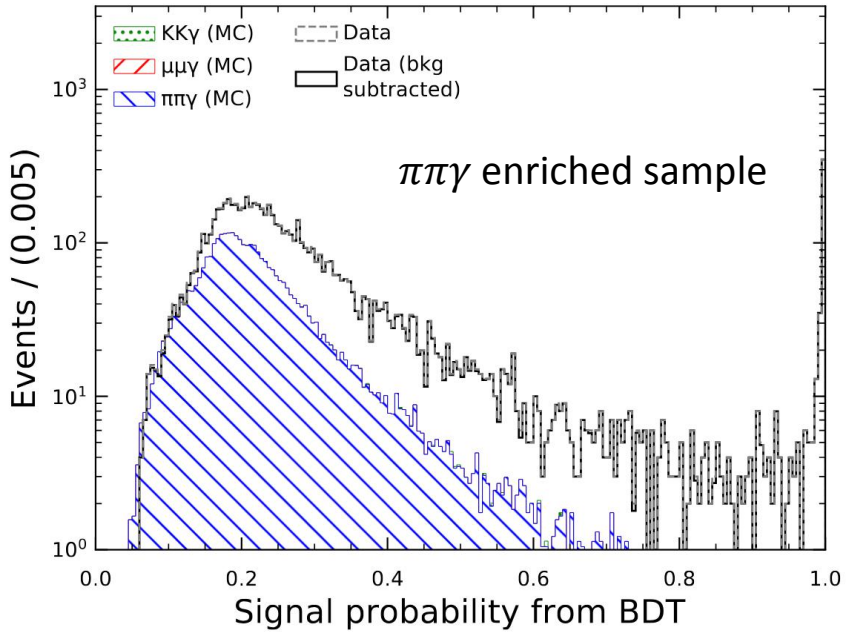

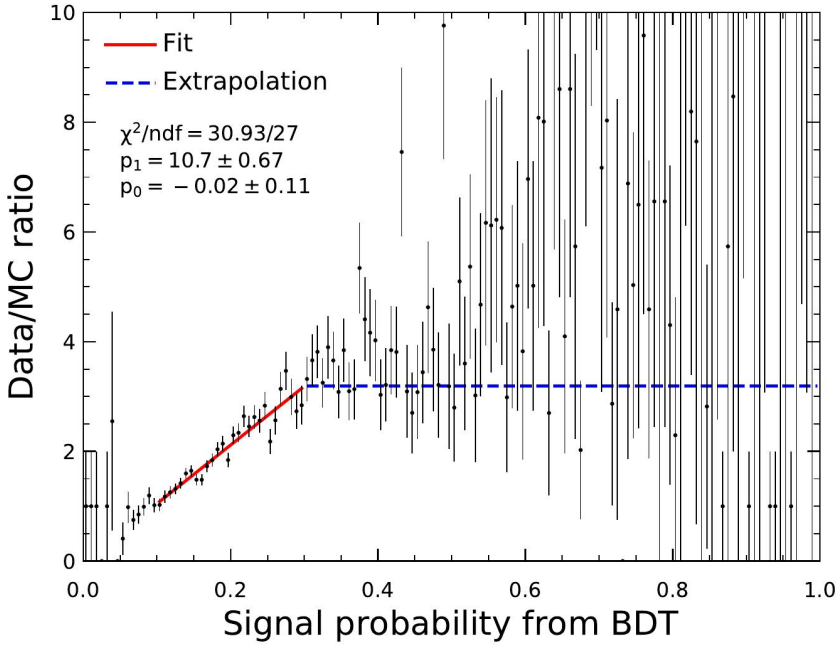

$ee\gamma$ background templates

Cut-based and BDT selections provide data-driven $ee\gamma$ sample.

$m_{\pi\pi}$: peak at threshold from $\gamma\gamma$ photon conversion, radiative Bhabha over the full range.

$|\cos\theta^*_\pi|$: peak at 1, less sharp at large masses. Increased bin size at small values to mitigate low statistics.

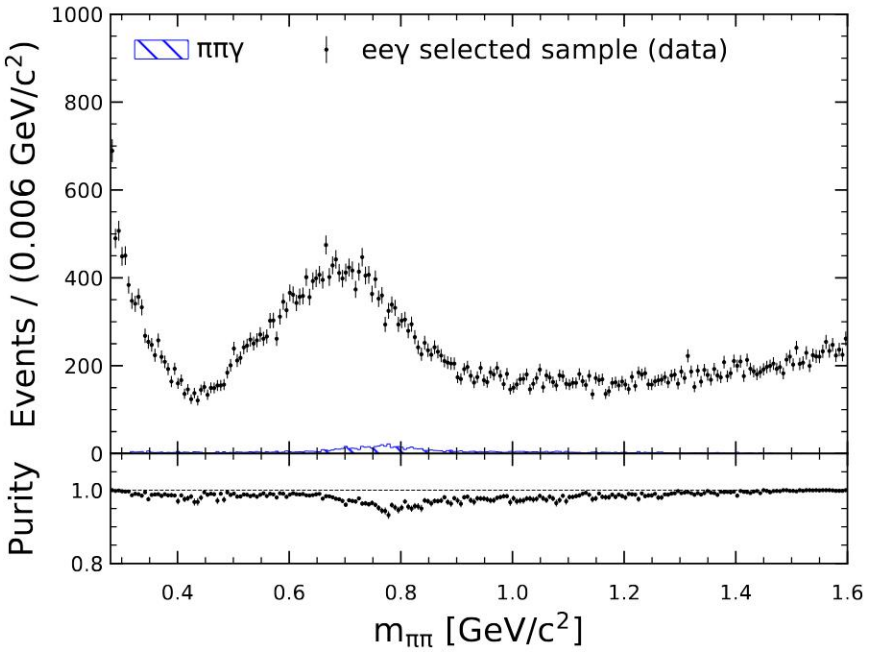

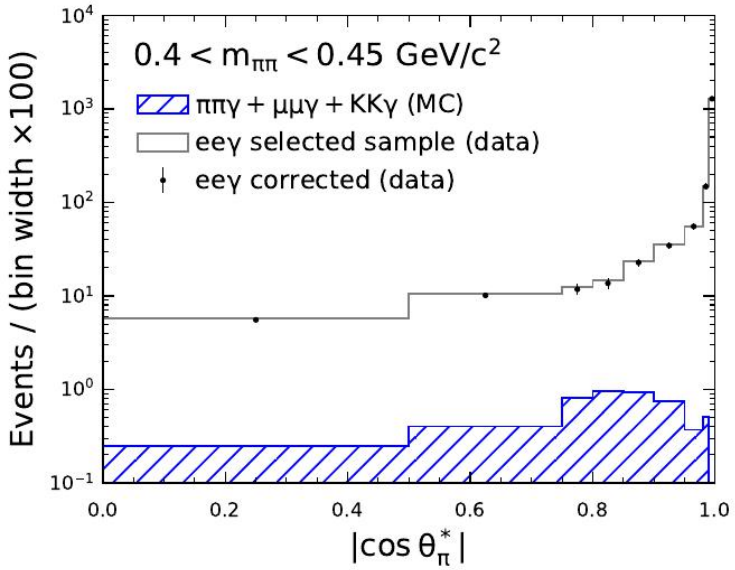

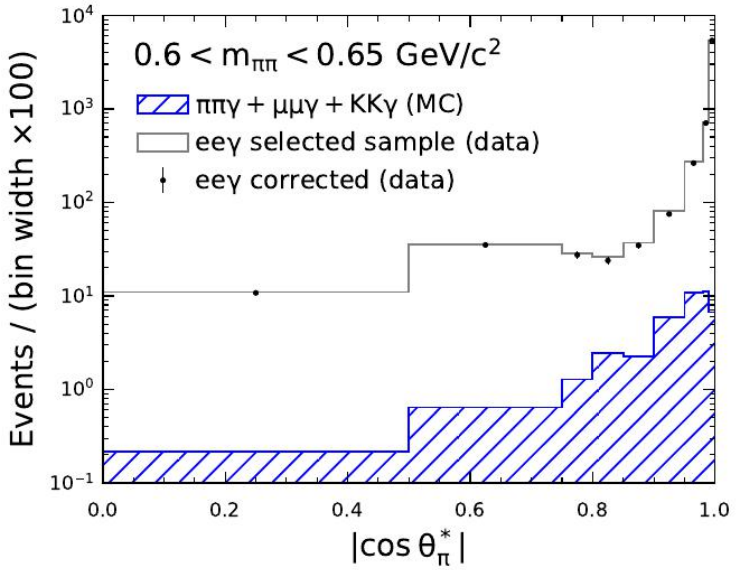

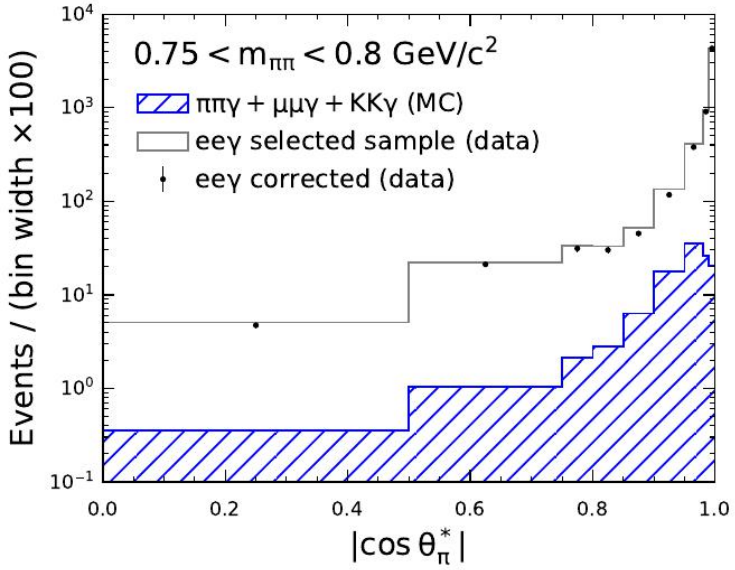

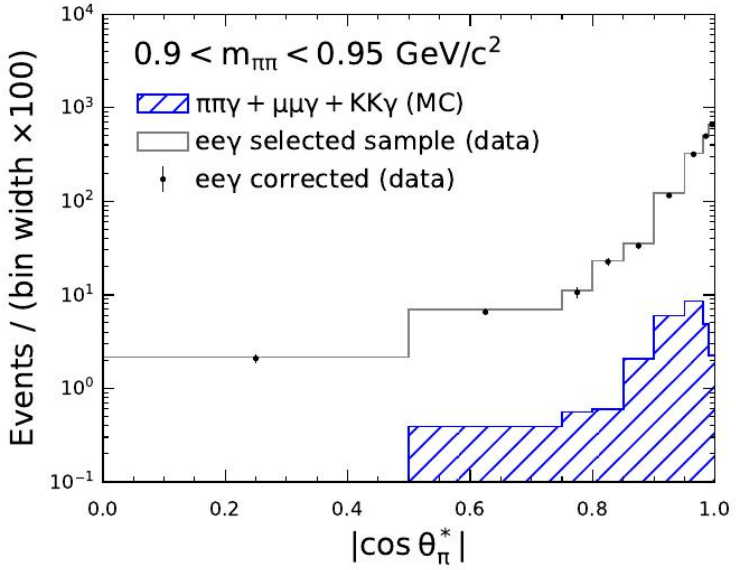

Uncertainties on $ee\gamma$ templates

2 sources of systematic uncertainties on $ee\gamma$ templates: choice of BDT selection cut + scaling of $\pi\pi\gamma$ background subtracted to $ee\gamma$ selected sample.

BDT cut value fluctuated up/downwards + $\pi\pi\gamma$ background either scaled or not scaled → comparison with nominal fit results gives systematic uncertainties.

Statistical errors evaluated with **bootstraps**: independent random Poisson weights (centered on 1) assigned to data and MC events, then fit performed up to 2nd step. Process repeated 1000 times.

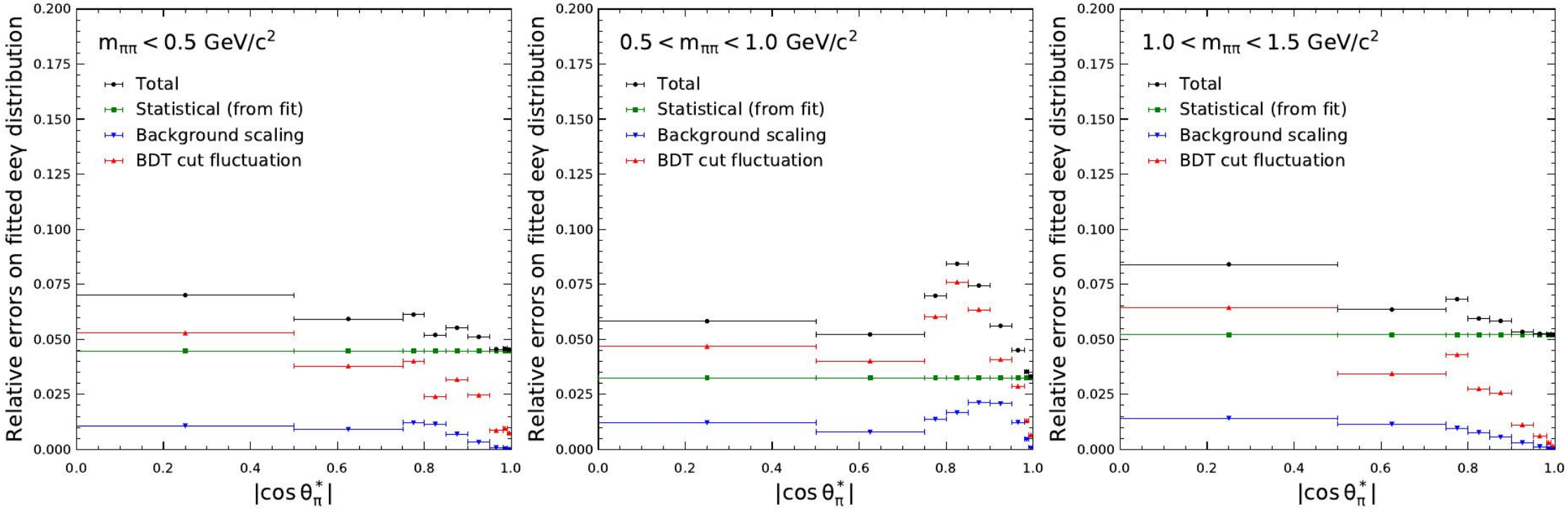

Impact of $ee\gamma$ systematics on mass spectra

Before fit between $|\cos\theta^*| = 0$ - 0.9, $ee\gamma$ is subtracted from data → $ee\gamma$ syst. error added in quadrature to data error.

Total relative error negligible in pion channel, below 2 per mil in muon channel
→ proves the effectiveness of the 3-step fit strategy.

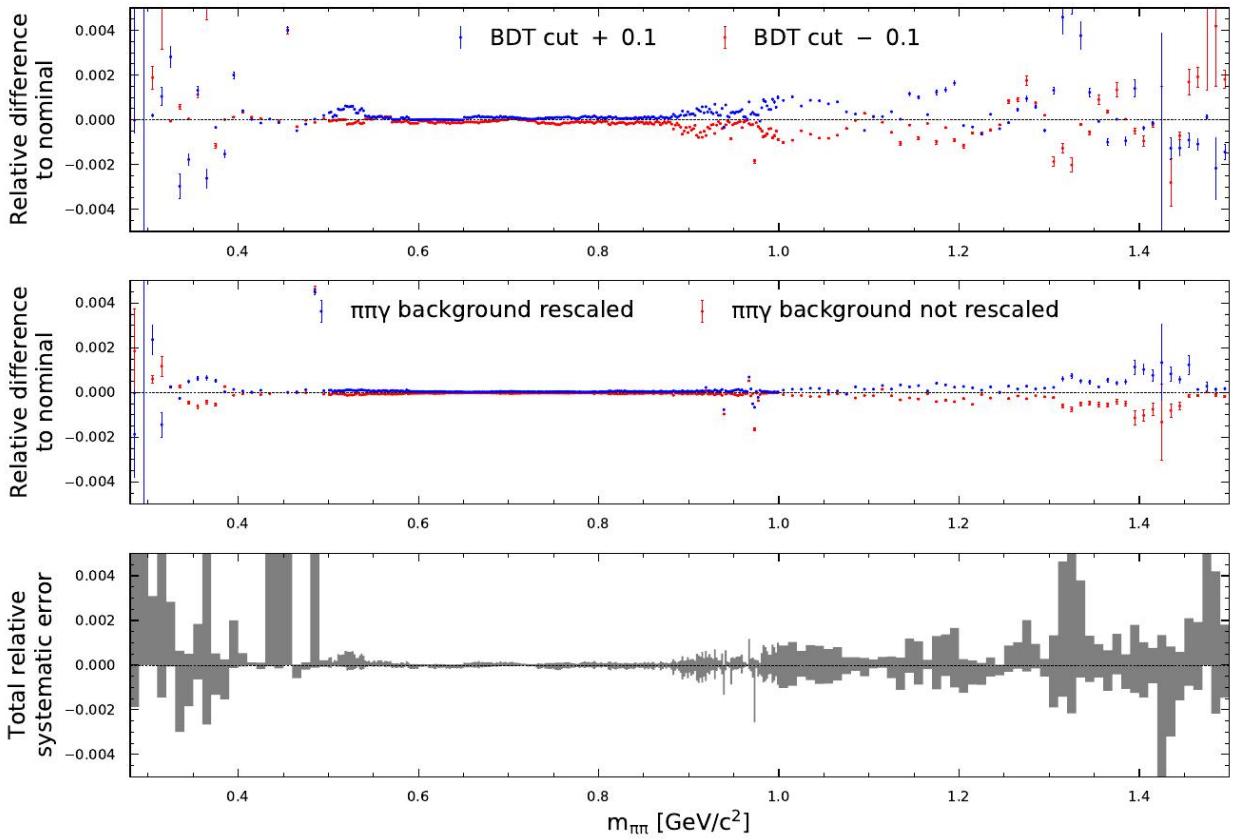

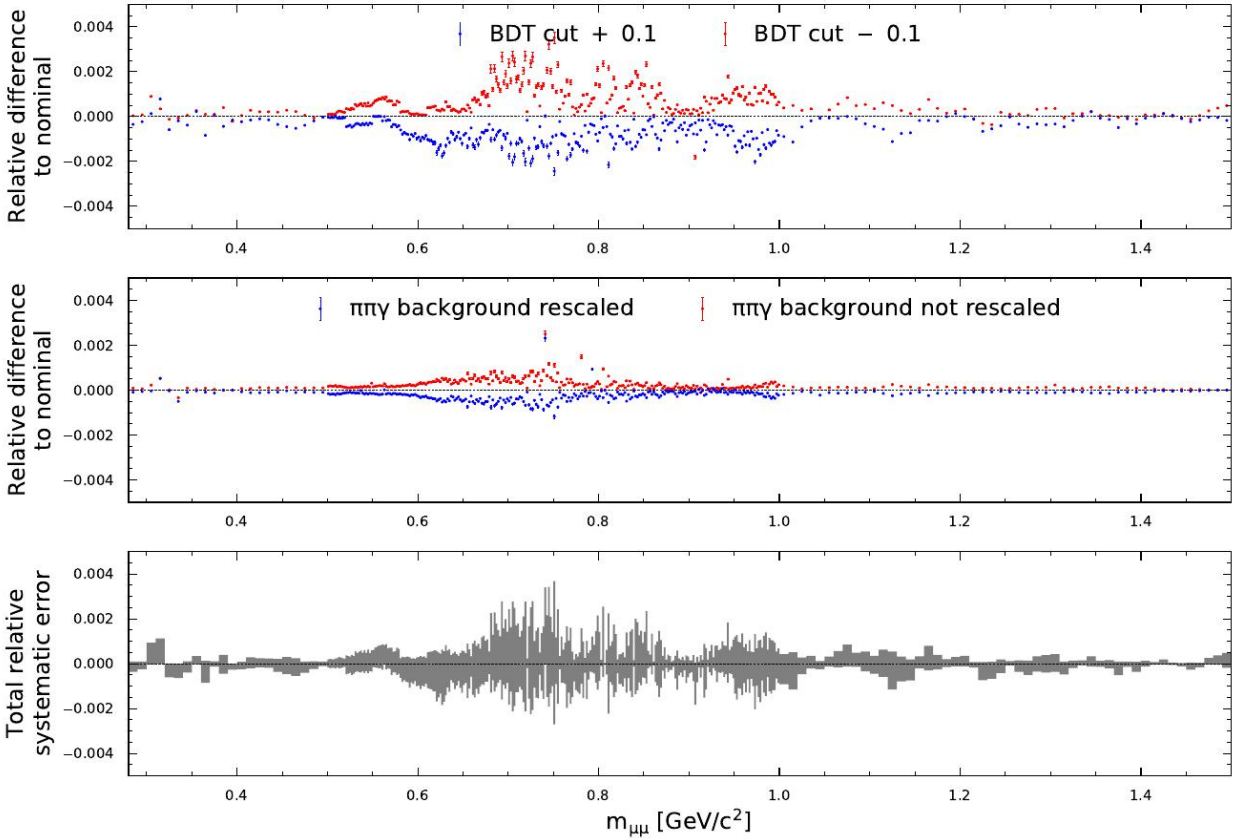

Accuracy of statistical uncertainties from the fit

Fit results compared to true $\pi\pi\gamma$ and $\mu\mu\gamma$ fractions with a **closure test** on MC events. Additionally, **bootstraps** (toys) generated to compare to statistical errors estimated by the fit.

Toys consistent with true fractions within uncertainties, with pull defined as $\frac{f_{\text{toys}}/f_{\text{true}} - 1}{\sigma_{\text{toys}}}$ (also the case for nominal fit).

Nominal fit tends to slightly underestimate (few % in relative) the statistical errors on the fitted fractions → toys used instead.

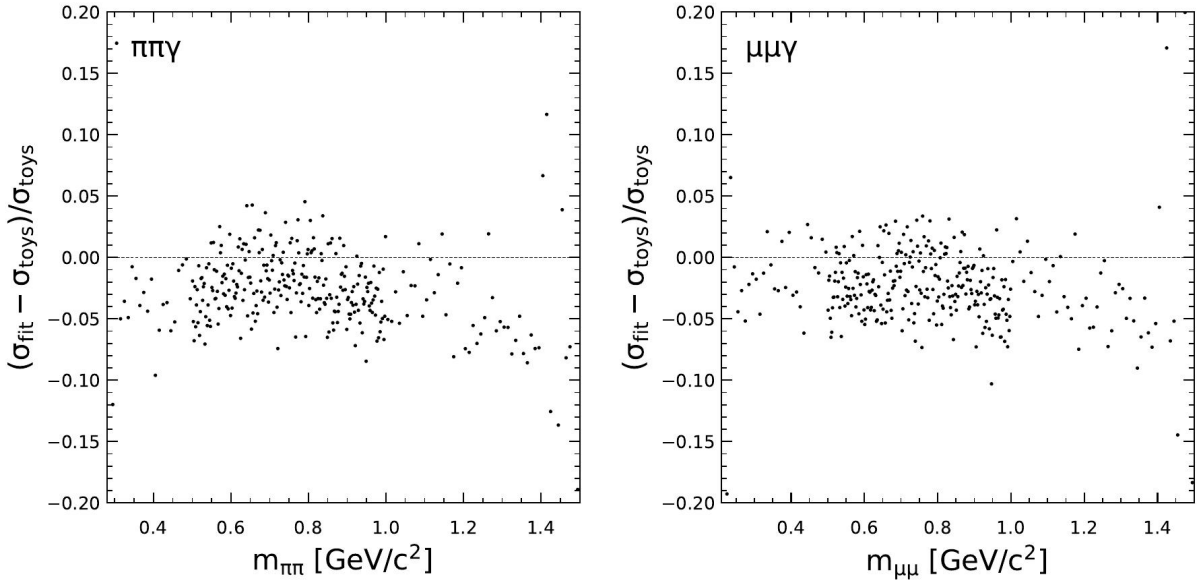

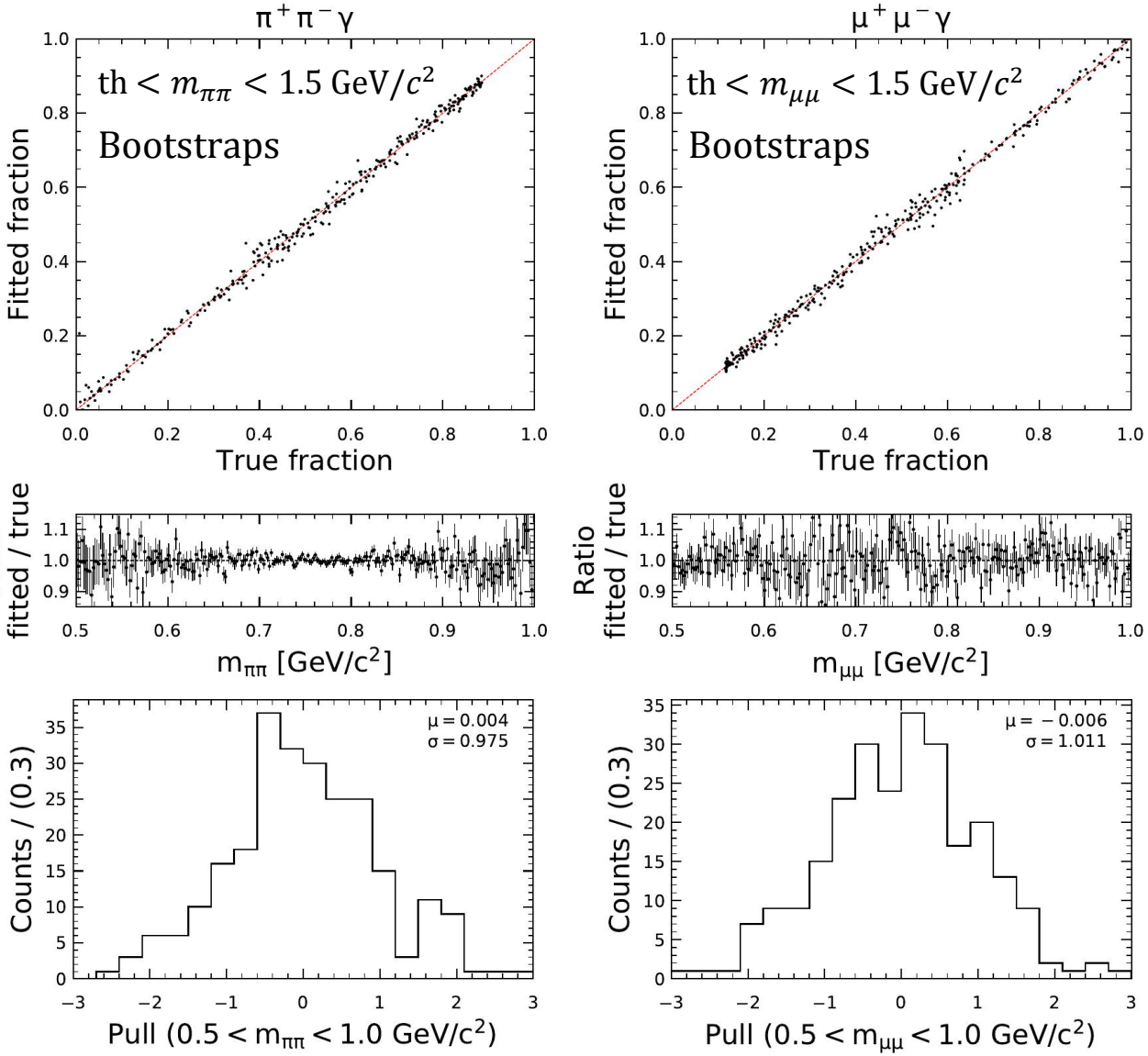

Accuracy of fitted fractions (1/2)

3 different test statistics considered for the fit:

$$\chi^2_{\text{Neyman}} = \sum_j \frac{(M_j - N_j)^2}{M_j + (\Delta N_j)^2}$$

- j : $|\cos\theta^*_\pi|$ bin,
- M_j : observed events (data),
- N_j : predicted events (fitted sum of templates),
- ΔN_j : statistical error on N_j.

$$\chi^2_{\text{Pearson}} = \sum_j \frac{(M_j - N_j)^2}{N_j + (\Delta N_j^{\text{fix}})^2}$$

1. a first fit with Neyman's χ^2,
2. four subsequent iterations (for convergence) with Pearson's χ^2 and ΔN_j^{fix} = fixed stat. error updated from previous iteration.

$$\chi^2_{\text{CNP}} = \sum_j \frac{(M_j - N_j)^2}{3/\left(\frac{1}{M_j+(\Delta N_j)^2} + \frac{2}{N_j+(\Delta N_j)^2}\right)}$$

X. Ji, W. Gu, X. Qian, H. Wei, C. Zhang
Combined Neyman-Pearson Chi-square: An Improved Approximation to the Poisson-likelihood Chi-square
NIMA 961, P163677 (2020)

designed to reduce the inherent biases of Neyman's and Pearson's χ^2.

$$N = M\left[\sum_{i=1}^{k-1} f_i x_i + \left(1 - \sum_{i=1}^{k-1} f_i\right) x_k\right] \pm M\sqrt{\sum_{i=1}^{k-1} (f_i \Delta x_i)^2 + \left[\left(1 - \sum_{i=1}^{k-1} f_i\right) \Delta x_k\right]^2}$$

M: integral over $|\cos\theta^*|$ of the fitted data distribution in a mass bin,

$f_i \in [0,1]$: parameters of fit, scale factors of templates with $\sum_i^k f_i = 1$.

Accuracy of fitted fractions (2/2)

3 methods investigated with a **closure test**: 10% of MC $\pi\pi\gamma$, $\mu\mu\gamma$ and $KK\gamma$ samples used in place of data, remaining 90% provide fit templates.

Bias expressed as the ratio of the fitted fraction to the true one, averaged over the 10 splittings and contiguous mass bins.

Performances of chi-squares compared as a function of $m_{\pi\pi}$ and $m_{\mu\mu}$: **CNP χ^2** gives the smallest biases everywhere except below 0.5 GeV/c^2 ($f_{\pi\pi\gamma}$ larger than 3%), used as test statistic of the fit.

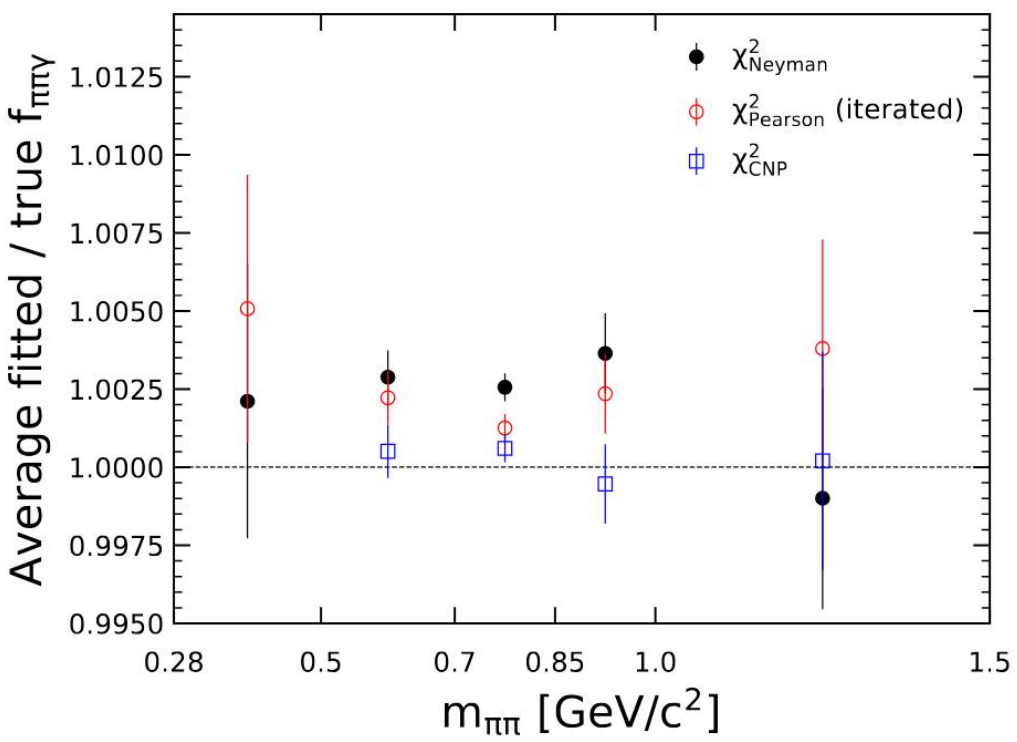

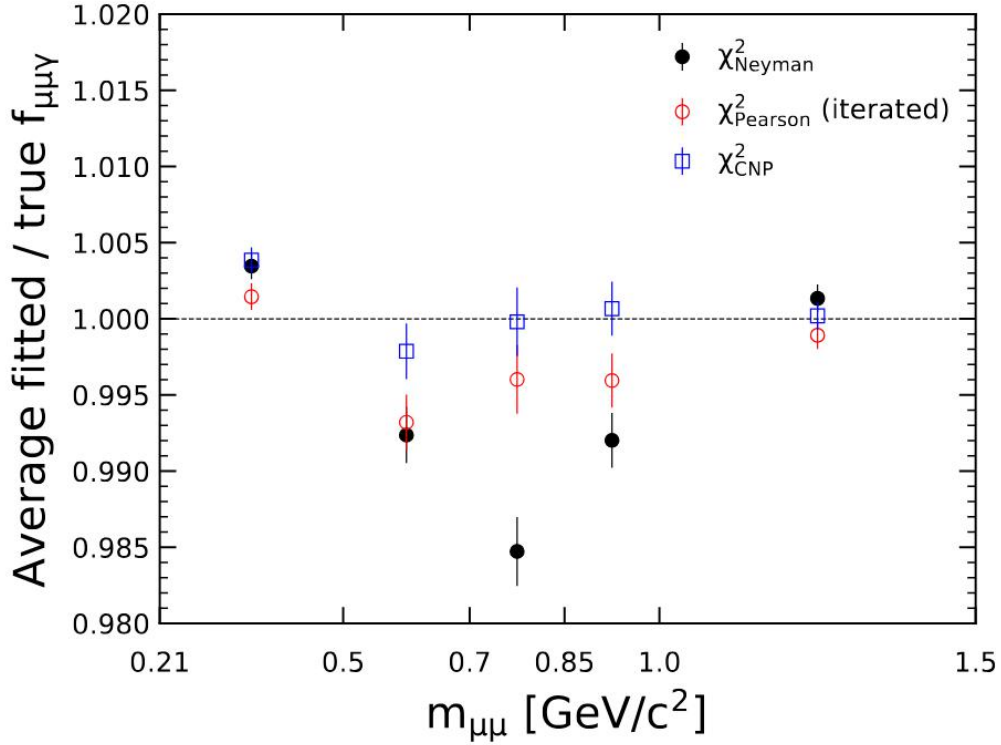

$\mu\mu\gamma$ mass spectrum basis (1/2)

Both $\pi\pi\gamma$ and $\mu\mu\gamma$ spectra must be measured with the corresponding mass hypotheses ($m_{\pi\pi}$ and $m_{\mu\mu}$).

With fits on $m_{\pi\pi}$ only, there are **2 options** for changing the basis to $m_{\mu\mu}$:

1. weight data events by the fraction of $\mu\mu\gamma$ in $m_{\pi\pi}$ bins according to the angular fit results, then draw the $m_{\mu\mu}$ distribution,
2. rely on simulation samples to determine a transformation matrix from $m_{\pi\pi}$ to $m_{\mu\mu}$.

Both options investigated with a **closure test**.

1st option: weights applied to pseudodata events defined as proportion of $\mu\mu\gamma$ events in 2D $m_{\pi\pi}$ vs $|\cos\theta^*_\pi|$ bins according to the fit.

Weighted distribution displays a peak between 0.35-0.4 GeV/c^2, not present in reconstructed MC spectrum
↪ different shift from $m_{\pi\pi}$ to $m_{\mu\mu}$ depending on the process, especially for $KK\gamma$.

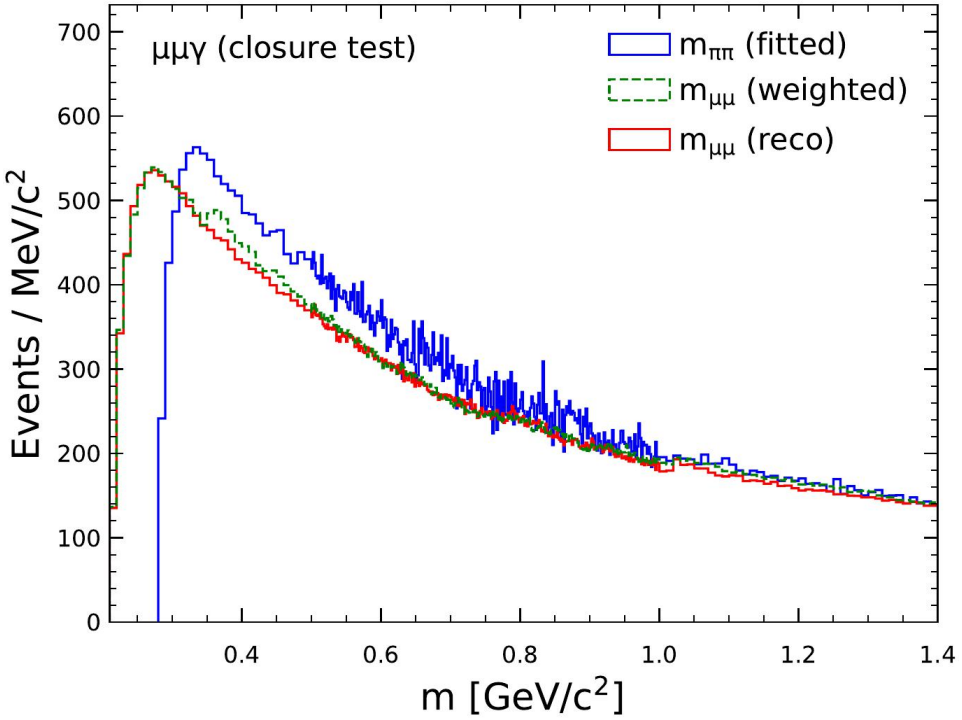

$\mu\mu\gamma$ mass spectrum basis (2/2)

2nd option: transformation matrix normalized in $m_{\pi\pi}$ bins and applied to shift the fitted $\mu\mu\gamma$ spectrum.

Agreement between reconstructed and shifted spectra depends heavily on the MC splitting (10 vs 90%),
below an example with 2 different pseudodata samples
↪ result on data unpredictable, therefore unreliable.

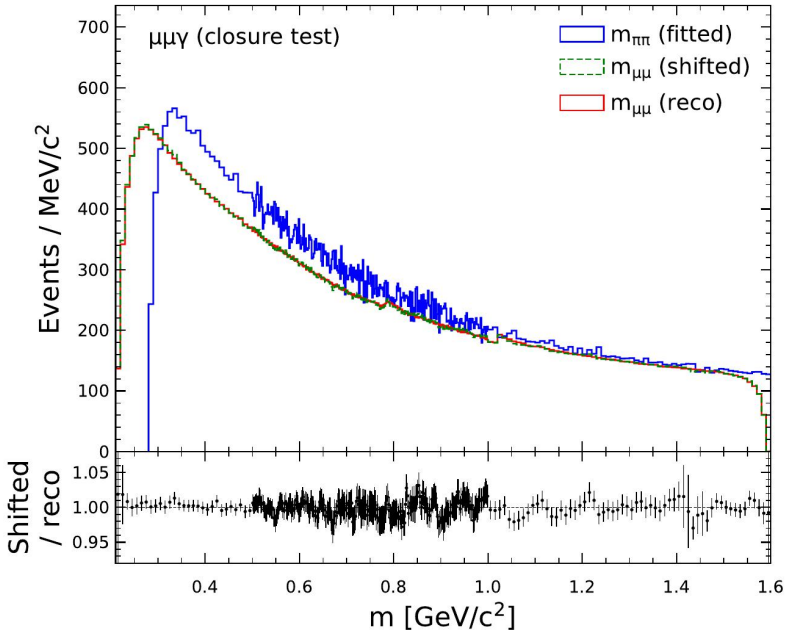

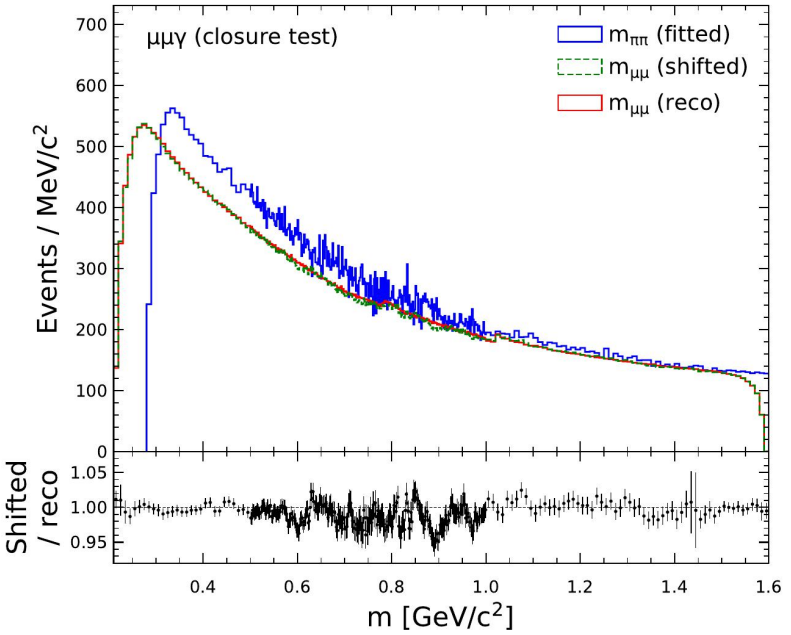

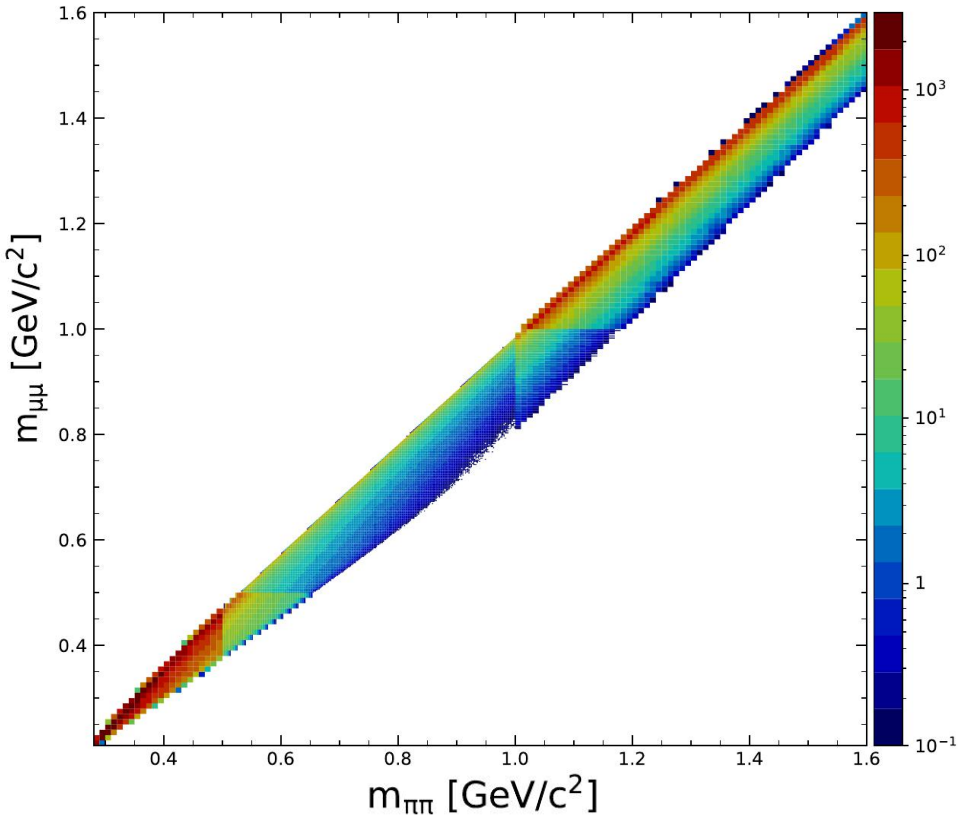

Angular fit in 4 representative mass bins

$m_{\pi\pi}$: 322 bins from 0.28 to 1.5 GeV/c².

$m_{\mu\mu}$: 329 bins from 0.21 to 1.5 GeV/c².

width: 2 MeV/c² bins between 0.5 - 1 GeV/c², 10 MeV/c² outside.

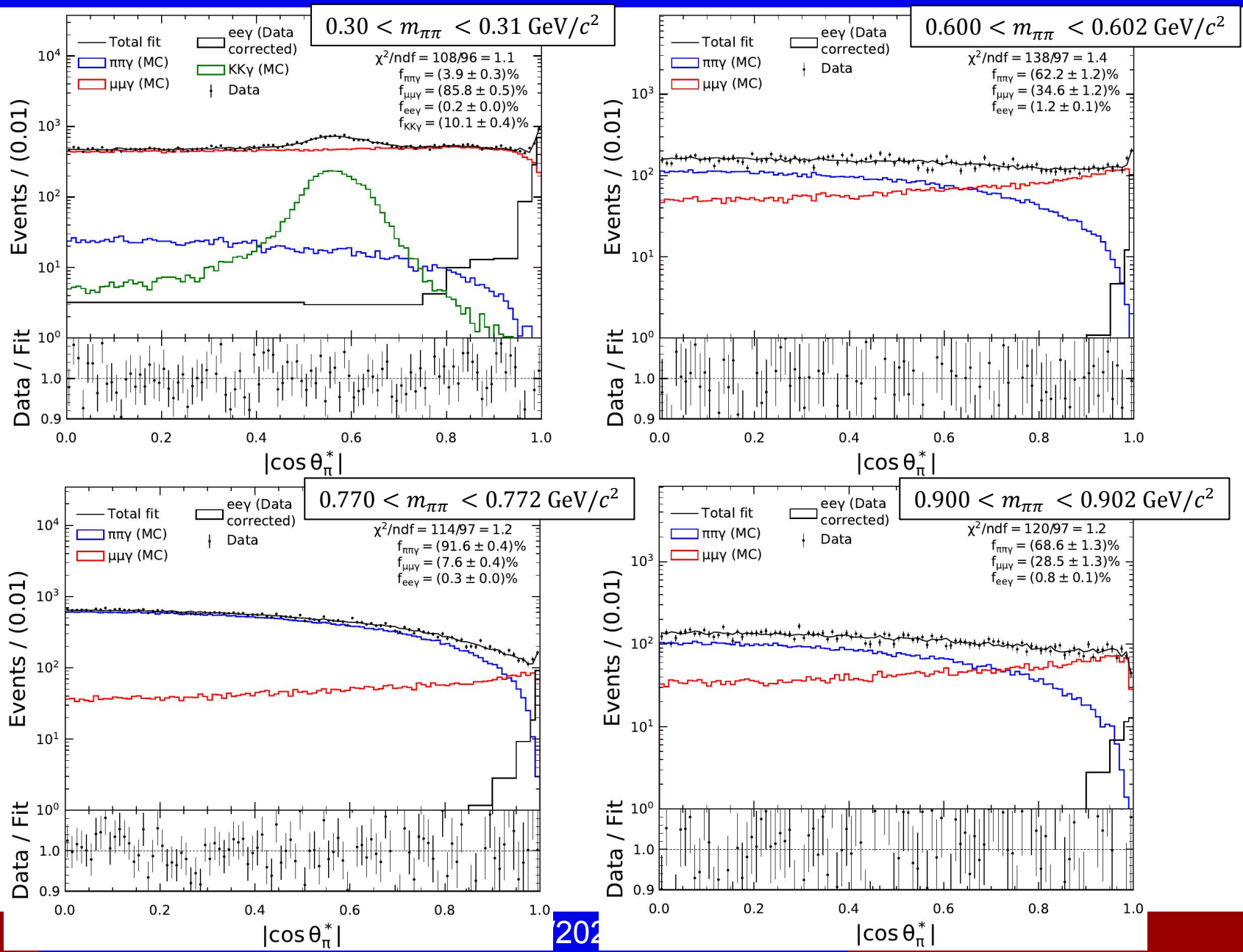

Corrections to simulation

Efficiency corrections determined for $|\cos\theta^*|$ templates and fitted masses due to:

- 2D-χ^2 selection,
- V_{xy} selection (distance between displaced vertex of two tracks and beam spot in transverse plane),
- trigger and tracking efficiencies,
- secondary interactions and fake photons (pions only).

Large effect of corrections on mass spectra (at most ±5% difference to uncorrected spectra), however they tend to cancel when combined.

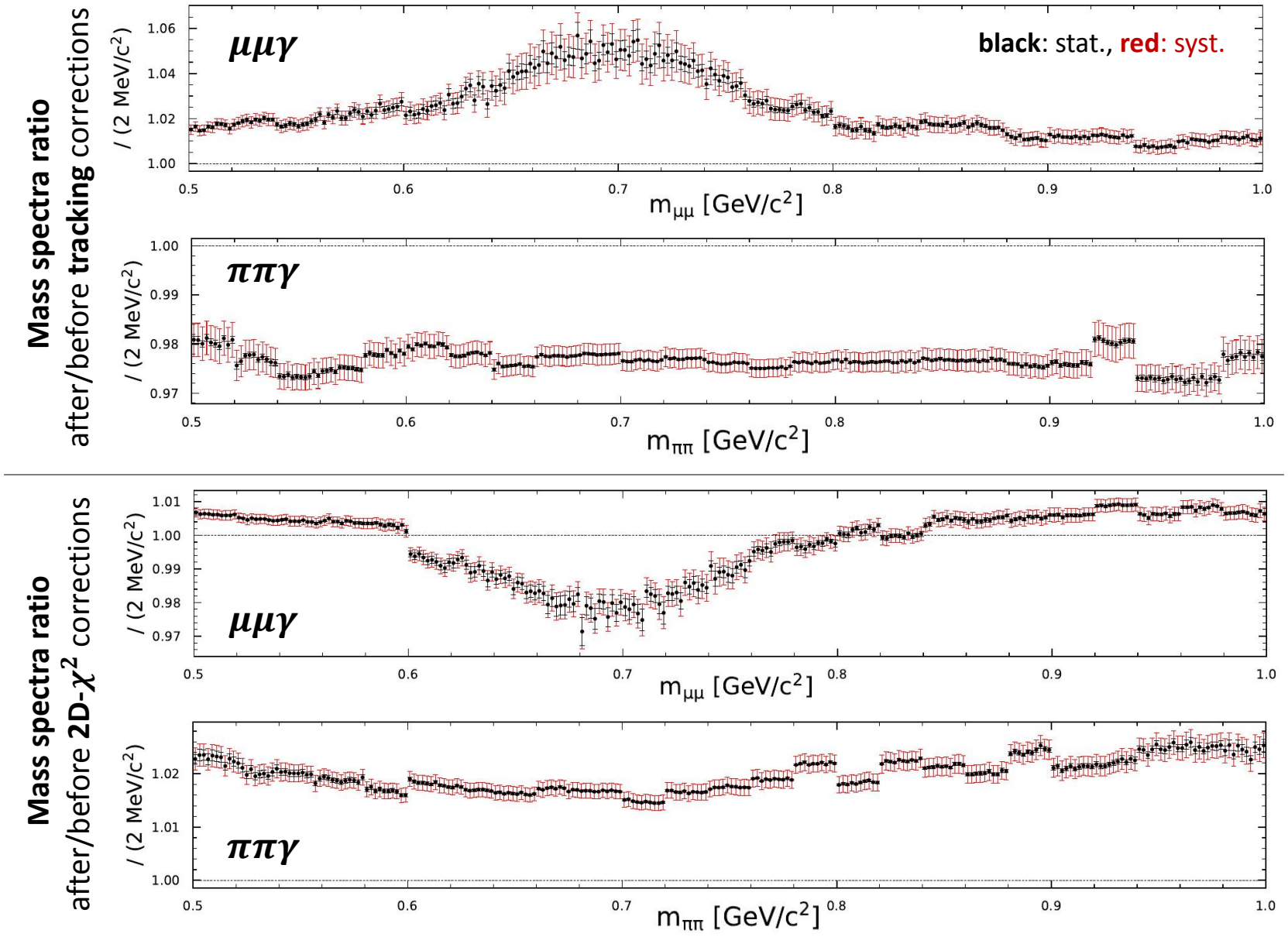

Unfolding of mass spectra

$m_{\pi\pi}$ and $m_{\mu\mu}$ masses unfolded to center-of-mass energy ***after*** $\boldsymbol{\gamma_{ISR}}$ ***is emitted*** $\rightarrow \sqrt{s'}$ = CM energy of $XX(\gamma)$ system ($X = \pi, \mu$), with possible additional FSR emitted by charged track, typically at large angle from beams.

Requires separation of FSR photons from LA ISR:
information not available in *Phokhara* generator because of ISR-FSR interference at NLO.
However, alternative generator *AfkQED* generates no LA ISR at NLO
⇒ minimum angle between additional γ_{LA} and charged tracks $\boldsymbol{\theta_{\mathbf{min(trk,\gamma_{LA})}}}$ fitted with FSR template (*AfkQED*) and LA ISR template (*Phokhara* - *AfkQED*).
FSR and LA ISR separation at 20 degrees.

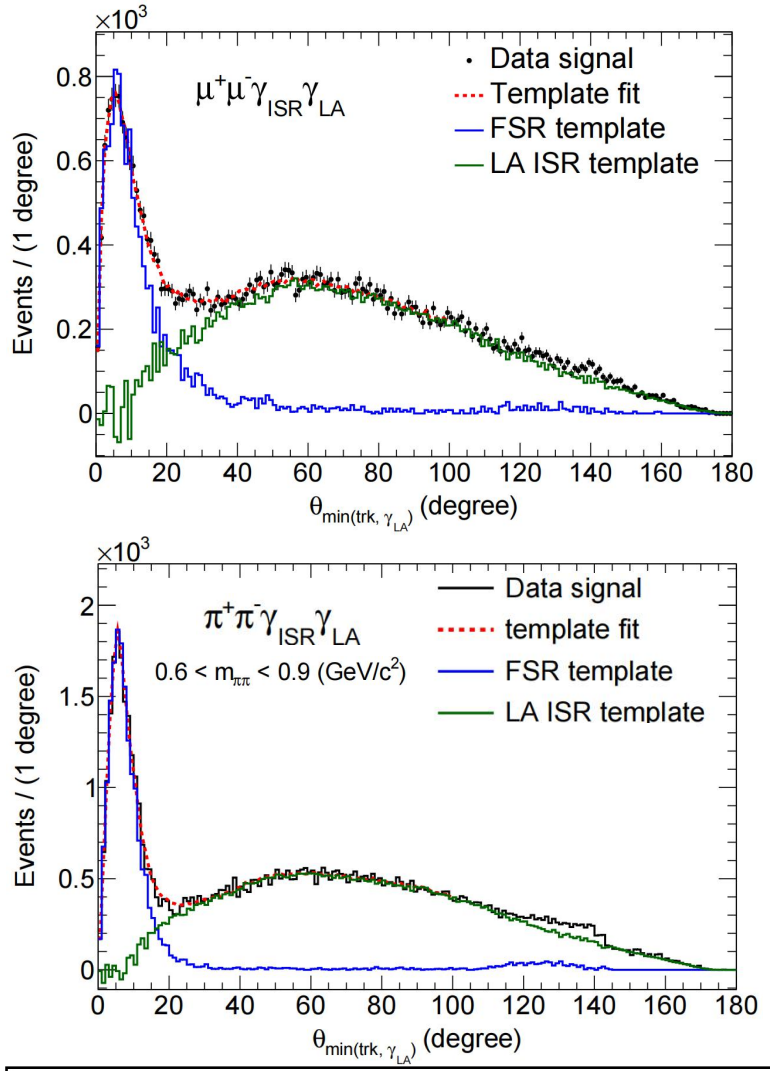

J. P. Lees *et al.* (BABAR Collaboration)
Measurement of additional radiation in the initial-state-radiation processes e+e−→μ+μ−γ and e+e−→π+π−γ at BABAR
Phys. Rev. D 108, L111103 – Published 21 December 2023

Unfolding of mass spectra

$m_{\pi\pi}$ and $m_{\mu\mu}$ masses unfolded to center-of-mass energy ***after γ_{ISR} is emitted*** $\rightarrow \sqrt{s'}$ = CM energy of $XX(\gamma)$ system ($X = \pi, \mu$), with possible additional FSR emitted by charged track, typically at large angle from beams.

<u>Requires separation of FSR photons from LA ISR</u>:
information not available in *Phokhara* generator because of ISR-FSR interference at NLO.
However, alternative generator *AfkQED* generates no LA ISR at NLO
⇒ minimum angle between additional γ_{LA} and charged tracks $\boldsymbol{\theta_{\mathbf{min(trk,\gamma_{LA})}}}$ fitted with FSR template (*AfkQED*) and LA ISR template (*Phokhara* - *AfkQED*).
FSR and LA ISR <u>separation at 20 degrees</u>.

⇒ $\sqrt{s'}$ computed on simulation with true information on charged tracks, adding possible photon if within 20° cone around a track.

⇒ provides 2D transfer matrix from m_{XX} to $\sqrt{s'}$, applied to data mass spectra.

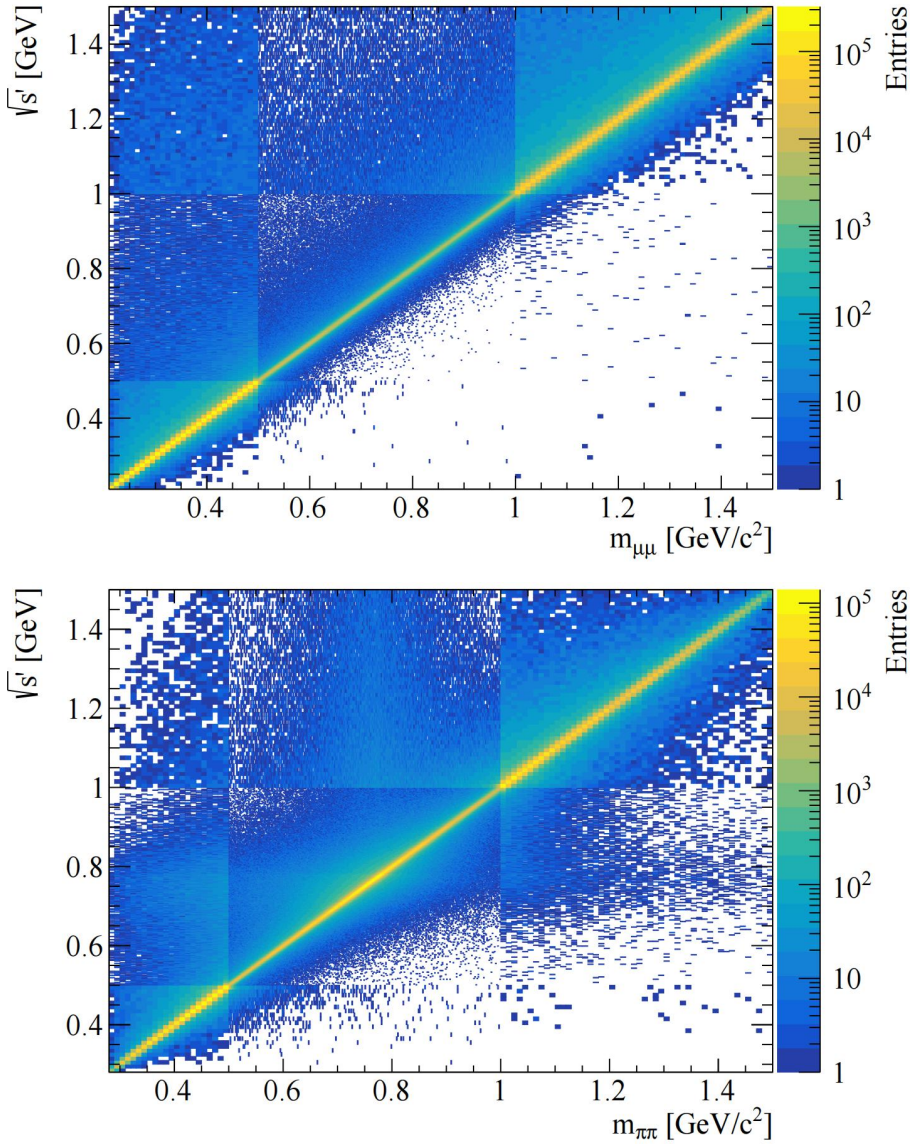

$\mu\mu\gamma$ spectrum comparison to QED prediction

$\mu\mu\gamma$ data spectrum can be compared to QED prediction, obtained by correcting the simulated *Phokhara* spectrum for:

- ISR photon efficiency difference with data,
- shortcomings related to overestimation of ISR "NLO" and absence of NNLO in *Phokhara*,
- imprecise description of vacuum polarization effects.

The data/QED ratio is fitted with a constant:

$$0.9955 \pm \underbrace{0.0035_{\text{stat}}}_{\substack{\textit{data + stat}\\\textit{errors on}\\\textit{corrections}}} \pm \underbrace{0.0030_{\text{fit}}}_{\substack{\textit{syst errors on}\\\textit{corrections}}} \pm \underbrace{0.0033_{\gamma\ \text{ISR}}}_{\substack{\textit{ISR photon}\\\textit{data/MC}\\\textit{efficiency}}} \pm \underbrace{0.0043_{\text{lumi}\ ee}}_{\substack{\textit{error on}\\e^+e^-\\\textit{luminosity}}}$$

compatible with unity within a precision of 0.71%

⇒ **validates the $\pi\pi/\mu\mu$ separation procedure.**

**** includes systematics + correlations***